NASA Contractor Report 166015

Advanced Manufacturing Development of a Composite Empennage Component for L-1011 Aircraft

PHASE V — FINAL REPORT
FULL SCALE GROUND TEST

A. Jackson, F. Dorward

LOCKHEED-CALIFORNIA COMPANY
BURBANK, CALIFORNIA

CONTRACT NAS1-14000

DECEMBER 1982

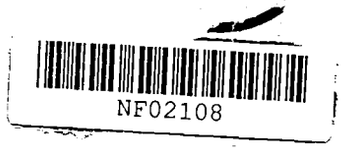

NASA
National Aeronautics and
Space Administration

Langley Research Center
Hampton, Virginia 23665

FOREWORD

This report was prepared by Lockheed-California Company under Contract NASI-14000, Advanced Manufacturing Development of a Composite Empennage Component for L-1011 Aircraft. It is the final report for the Phase V - Ground Tests activity covering work completed between 1 September 1979 and 27 August 1982. This work is sponsored by the National Aeronautics and Space Administration (NASA) Langley Research Center. The program managers for Lockheed were Mr. Fred C. English and Mr. W.F. Priest. Mr. Herman L. Bohon is project manager for NASA Langley. The technical representative for NASA Langley is Dr. Herbert A. Leybold.

Engineering Development activity (Phase I) is reported in NASA CR-144986. Design Analysis activity (Phase II) is reported in NASA CR-165634, and Manufacturing Development activity (Phase IV) is reported in NASA CR-165885. The final phase still to be reported is the Production Readiness Verification Tests (Phase III), which is scheduled for completion in September 1983.

The following Lockheed personnel were principal contributors to the program during Phase V:

A.C. Jackson	Engineering Manager
F. Dorward	Structural Test
C.S. Oswell	Structural Test
J.H. Burrell	Structural Test
W.F. Bush	Structural Test
R.L. Lowe	Structural Test
T. Gillette	Structural Test
R.A. Meyer	Instrumentation
B.P. Perrine	Instrumentation
R.R. Van Cleave	Stress
M.A. Quan	Stress
S.R. Nanning	Stress
H.J. Roffelson	Design
R.C. Crane	Test Fixture Fabrication
K.M. Le Duc, B. Mosesian	Quality Assurance Managers
M.J. Berg	Non-destructive Inspection

Page Missing in Original Document

TABLE OF CONTENTS

TABLE OF CONTENTS (Continued)

LIST OF FIGURES

LIST OF FIGURES (Continued)

LIST OF FIGURES (Continued)

Page Missing in Original Document

LIST OF TABLES

ADVANCED MANUFACTURING DEVELOPMENT OF A COMPOSITE EMPENNAGE COMPONENT FOR L-1011 AIRCRAFT

PHASE V FINAL REPORT FULL SCALE GROUND TESTS

A.C. Jackson and F. Dorward

SUMMARY

This is the final report of the Ground Tests (Phase V) conducted on the Advanced Composite Vertical Fin (ACVF) program. The significant elements of this program phase include the design and fabrication of the test fixture and the transition structure, static test of Ground Test Article (GTA) No. 1, rework of GTA No. 2, and static, damage tolerance, fail-safe and residual strength tests of GTA No. 2.

GTA No. 1 failed during static test at 98 percent Design Ultimate Load (DUL). The failure was due to a combination of loads which applied interlamina tension and bending to the front spar cap. Subsequent tests showed that the spar cap had very low strength capability in interlamina tension and that a low cycle high load fatigue spectrum during the pretest strain surveys caused a significant drop in strength.

GTA No. 2 was reinforced and tested to complete the ground test program. Testing commenced with a static test to 106 percent DUL. The additional 6 percent was to cover environmental effects which were not simulated.

Impact damage was then inflicted at four locations on the left hand cover and one on the front spar web. Damage was visible to the eye at four of the five locations. One lifetime of damage tolerance testing was performed, representing 36,000 flights of spectrum fatigue loadings. Nondestructive inspection was performed each 1/4 lifetime. Some damage growth occurred at all locations, primarily in the first 1/2 lifetime.

Major damage was then inflicted to the left hand cover to simulate lightning strike damage. The damage included skin penetration and stiffener delamination and covered an area of approximately 12 in. by 4 in. A complete cycle of ±106 percent of limit load was applied. Post-test inspection showed no growth of this damage or the other five impact damaged areas.

The major damage was then repaired by bonding on a graphite/epoxy external patch and installing fasteners through the flanges of the two stiffeners in the damaged area. A second lifetime of damage tolerance testing was then accomplished. A post-test inspection again showed no changes at any of the damage locations.

Two of the initial five impact damage areas were then repaired in order to to preclude failures initiating in those two locations during the residual strength test.

The residual static strength test was then performed. Failure occurred at 120 percent DUL in the tension cover.

INTRODUCTION

The broad objective of the Aircraft Energy Efficiency (ACEE) Composite Structures Program is to accelerate the use of composite structures in new aircraft by developing technology and processes for early progressive introduction of composite structures into production commercial transport aircraft. This program, as one of several which are collectively aimed toward accomplishing that objective, has the specific objective to develop and manufacture advanced composite vertical fins for L-1011 transport aircraft. Laboratory tests and analyses have been made to substantiate that the composite fin can operate safely and economically under service loads and environments and will meet Federal Aviation Administration (FAA) requirements for installation on commercial aircraft. A limited quantity of units are being fabricated to establish manufacturing methods and costs. The Advanced Composite Vertical Fin (ACVF) consists of over 76 percent advanced composite materials and weighs about 27 percent less than the metal fin it replaces. A method was developed to establish cost/weight relationships for the elements of the composite and metal fins to establish cost-effective limits for composite applications.

The ACVF being developed under this program consists of the entire main box structure of the vertical stabilizer for the L-1011 transport aircraft. The box structure extends from the fuselage production joint to tip rib and includes the front and rear spars. It is 25 feet tall with a root box chord of 9 feet and represents an area of 150 square feet.

The primary objective of this program is to gain a high level of confidence in the structural integrity and durability of advanced composite primary structures. An important secondary objective is to gain sufficient knowledge and experience in manufacturing aircraft structures of advanced composite materials to assess properly their cost effectiveness.

The duration of this program is 88 months, with completion scheduled for November 1983. The master schedule for this program is shown on Figure 1. The program is organized in four overlapping phases: Phase II, Design and Analysis; Phase III, Production Readiness Verification Tests (PRVT); Phase IV, Manufacturing Development; and Phase V, Ground Tests. Phase I was completed during 1976.

The Lockheed-California Company has teamed with the Lockheed-Georgia Company in the development of the ACVF. Lockheed-California Company, as prime contractor, has overall program responsibility and has designed and fabricated

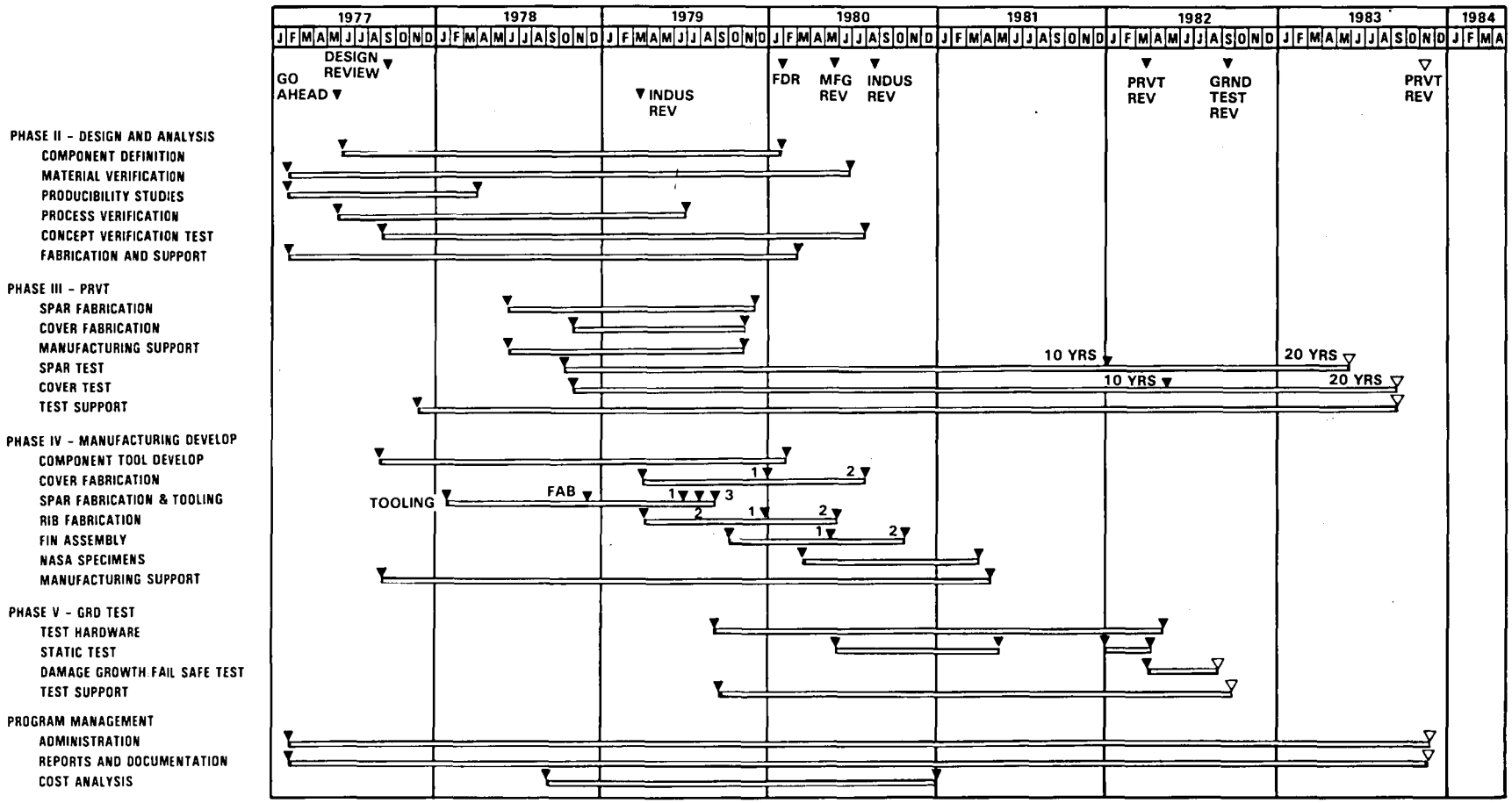

Figure 1. - ACVF program master schedule.

the covers and the ribs, has conducted the full-scale ground tests and is conducting the PRVT program. Lockheed-Georgia Company has designed and fabricated the front, rear, and auxiliary spars, and has assembled the composite fin at Lockheed's plant in Meridian, Mississippi, where the present L-1011 vertical fins are assembled.

Phase I, Engineering Development; Phase II, Design and Analysis; and Phase IV, Manufacturing Development have been completed and Phase III is in progress. Phase V has been completed and is reported here.

Phase III, Production Readiness Verification Tests (PRVT) are designed to provide information to answer the following questions:

- What is the range of production qualities that can be expected for components manufactured under conditions similar to those expected in production, and how realistic and effective are proposed quality levels and quality control procedures?

- What variability in static strength can be expected for production quality components, and are the margins sufficient to account for this variability?

- Will production quality components survive extended time laboratory fatigue tests involving both load and environment simulation of sufficient duration and severity to provide confidence in in-service durability?

To accomplish these objectives 22 components of each of two key structural elements of the ACVF were fabricated for test. One element represents the front spar/fuselage attachment area, and the other element represents the cover/fuselage joint area. Ten of each element have been static strength tested. Six of each element have been durability tested for the equivalent of ten years of service and will be statically tested at NASA Langley Research Center to determine their residual strengths. The remaining six of each will continue testing until the equivalent of 20 years of service has been accomplished. Two of each of these last six are durability tested at strain levels 1.5 times those in the basic program. All elements remaining at the completion of 20 years will be statically tested at NASA Langley Research Center to determine their residual strengths.

Throughout this program, technical information gathered during performance of the contract is being disseminated throughout the aircraft industry and to the government. This information is being distributed through quarterly reports that coincide with calendar quarters and final reports at the completion of each phase. All test data and fabrication data are being recorded on Air Force Data Sheets for incorporation in the Air Force Design Guide and Fabrication Guide

for Advanced Composites. Oral reviews have been conducted to acquaint the aircraft industry and the Government with progress of the program.

Use of commercial products or names of manufacturers in this report does not constitute official endorsement of such products or manufacturers, either expressed or implied, by the National Aeronautics and Space Administration

ABBREVIATIONS

GTA	Ground Test Article
DUL	Design Ultimate Load
DLL	Design Limit Load
ACVF	Advanced Composite Vertical Fin
PRVT	Production Readiness Verification Testing
VSS	Vertical Stabilizer Station
CDS	Central Data System
Gr/Ep	Graphite/Epoxy

1. COMPONENT DESCRIPTION

The fin box consists of 2 covers, 2 main spars, 1 stub spar and 11 ribs. Figure 2 shows an exploded view of the box. A brief description of the component is given below. A more detailed description is presented in Reference 1.

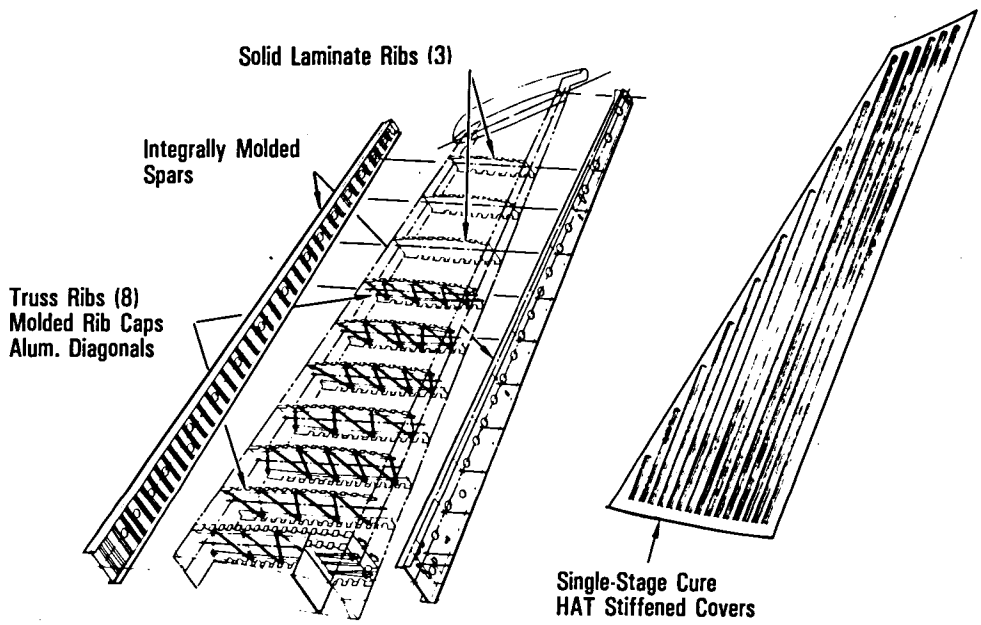

Figure 2. - ACVF design configuration.

1.1 Covers

The covers are designed primarily by stiffness. The composite fin box is designed to match the bending and torsional stiffness of the metal fin; the root end has to match the existing joint to the afterbody; and all interfaces are unchanged. The ($\pm 45^{o}$, 0^{o}) cover skin tapers in steps from 34 plies at the root end to 16, 14, then 10 plies. The edges are built up to 0.12 in., 24 plies, to allow for countersinking holes without feather edges. A thickness map is shown in Figure 3.

The covers are stiffened with co-cured hat sections. The stiffener is built up of two 5-ply segments with a 10-ply segment sandwiched between them in the crown. A short segment of eight doubler plies is added only at the root end to stiffen the side walls for shearing out the crown loads. Internal clips consisting of two plies at ±45 degrees are added for additional peeling strength.

The eleven ribs fall into three basic categories: The two lower ribs are actuator ribs, the next six are truss ribs, and the upper three are solid web ribs.

The actuator ribs consist of a solid graphite web stub rib at VSS 90.19 and a combination solid graphite web and graphite cap aluminum truss rib at VSS 97.19 shown in Figure 4. The solid web is a 16-ply layup $(+45/0/-45/90_2/$

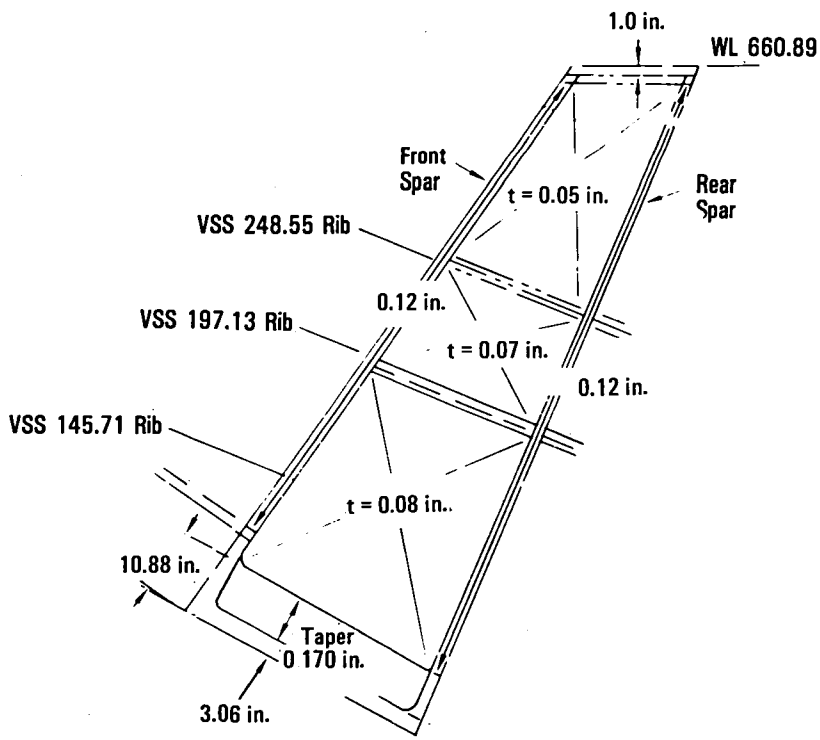

Figure 3. - Cover thickness.

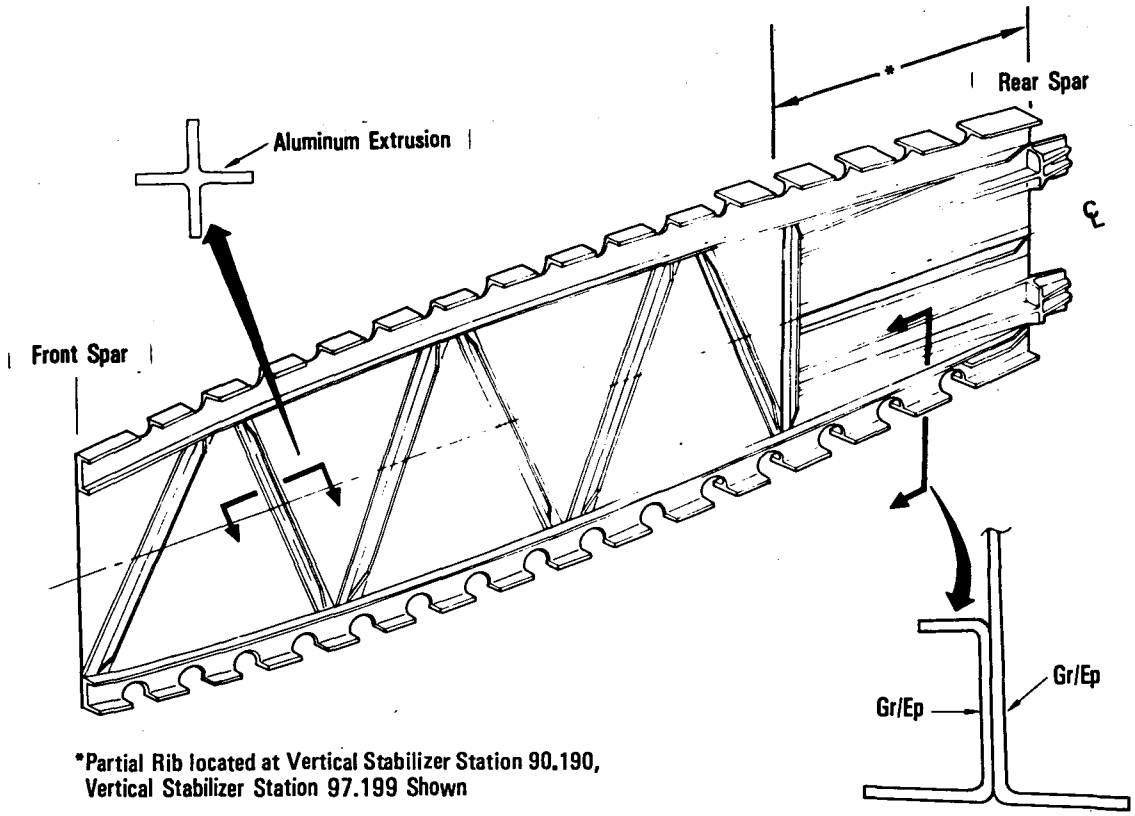

Figure 4. - Actuator rib.

$-45/0/+45)_s$. The sides adjacent to the covers are flanged to provide part of the skin attachment. Additional cap is provided by a C-section consisting of a 19-ply layup $(\pm45/90/\pm45/0/\pm45/0_3)_s$. This cap extends the full length on VSS 97.19. The forward portion of this rib consists of the graphite/epoxy C-section caps and aluminum cruciform extruded truss members.

The truss rib caps are C-section caps consisting of 19 plies with the same layup as the VSS 97.19 cap. The truss members are again aluminum cruciform extrusions. A typical truss rib is shown in Figure 5.

The solid web ribs are a sandwich design, with 0.03 in. syntactic core. Syntactic epoxy is an epoxy system filled with glass microballoons which has about half the density of graphite epoxy. The face sheets consist of seven plies laid up as $\pm45/0/90/0/\mp45$. The edges around the core are graphite epoxy laid up as $\pm45/0_2/\pm45$. The configuration of the solid web rib is shown in Figure 6.

1.3 Spars

Front and rear spars have been designed to comply with overall program objectives of providing at least a 20-percent weight savings over the metallic design, while maintaining production costs and ensuring structural and functional interchangeability with the baseline article.

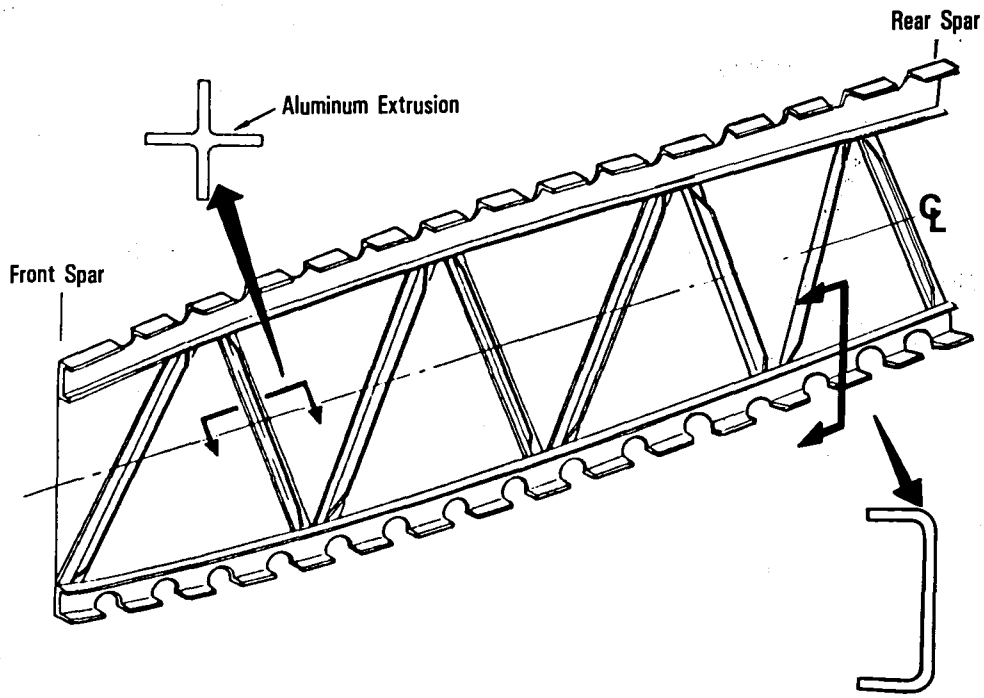

Figure 5. - Typical rib design.

The design concepts selected are the graphite/epoxy configurations shown in Figures 7 and 8. The front and rear spars are similar in shape and size and are basically one-piece components with rib attach angles, stiffeners, caps, and webs integrally molded in a single cocured operation. The front spar cap forward flange, rear spar cap aft flange, and the fuselage joint areas have been configured to interface with the existing metallic structure.

Strength and stiffness requirements are controlled by selecting ply layups with a sufficient number of ±45-degree plies in the webs to provide the required shear strength and 0-degree plies in the caps for axial loading. To facilitate fastener installation in the final assembly fixture, access holes have been provided in the spar webs. Two access holes are required in each rib bay, and this dictates that three web stiffeners are added between ribs to ensure uniform hole spacing. The access hole edges are not reinforced.

The stub spar shown in Figure 9 is located between the aft fuselage closure rib and the rudder actuator rib, and has been retained as an aluminum assembly.

1.4 Box Assembly

Vertical fins for the ACVF program were assembled at the Lockheed-Georgia Company facility in Meridian, Mississippi, using an existing assembly fixture

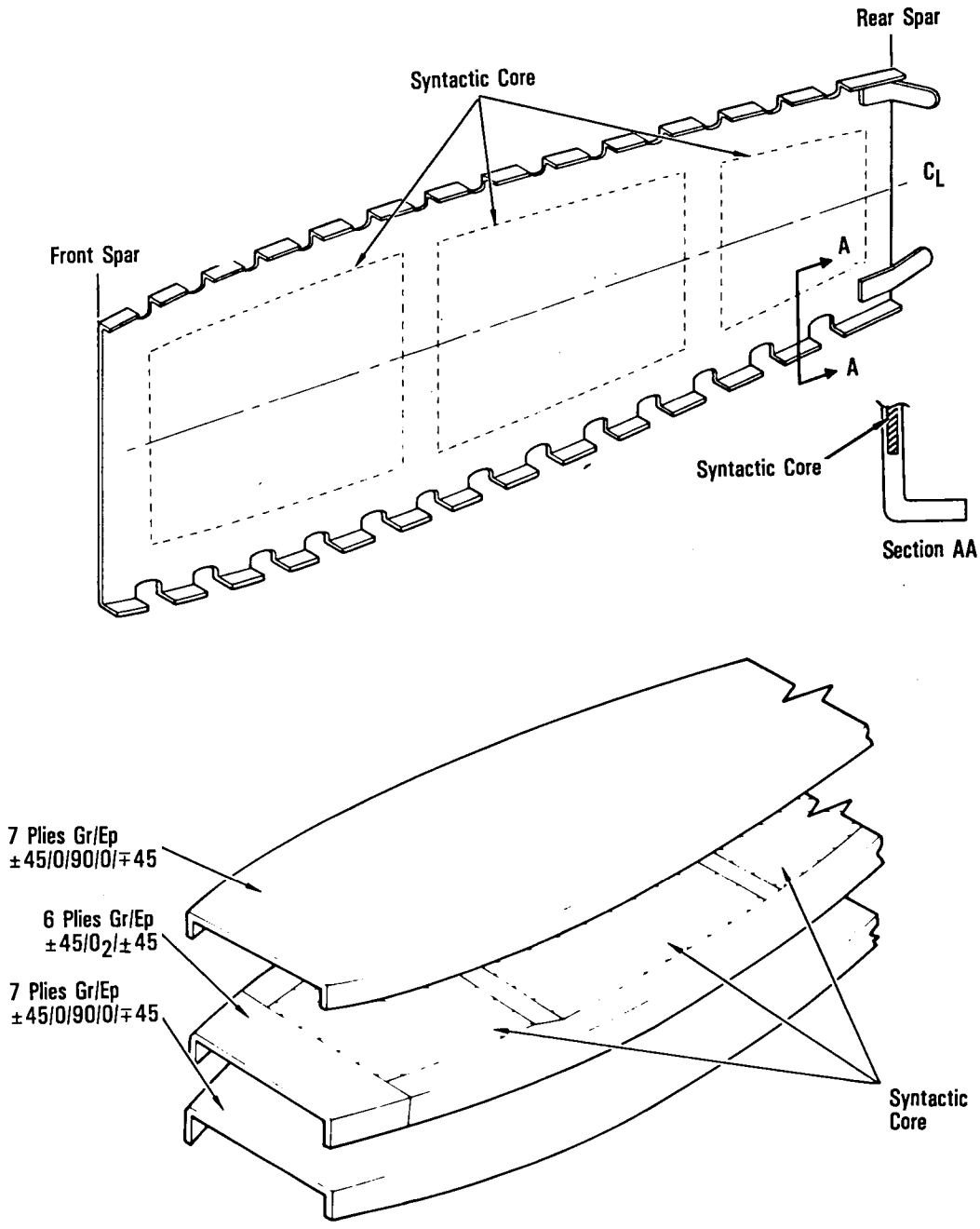

Figure 6. - Typical solid web rib design.

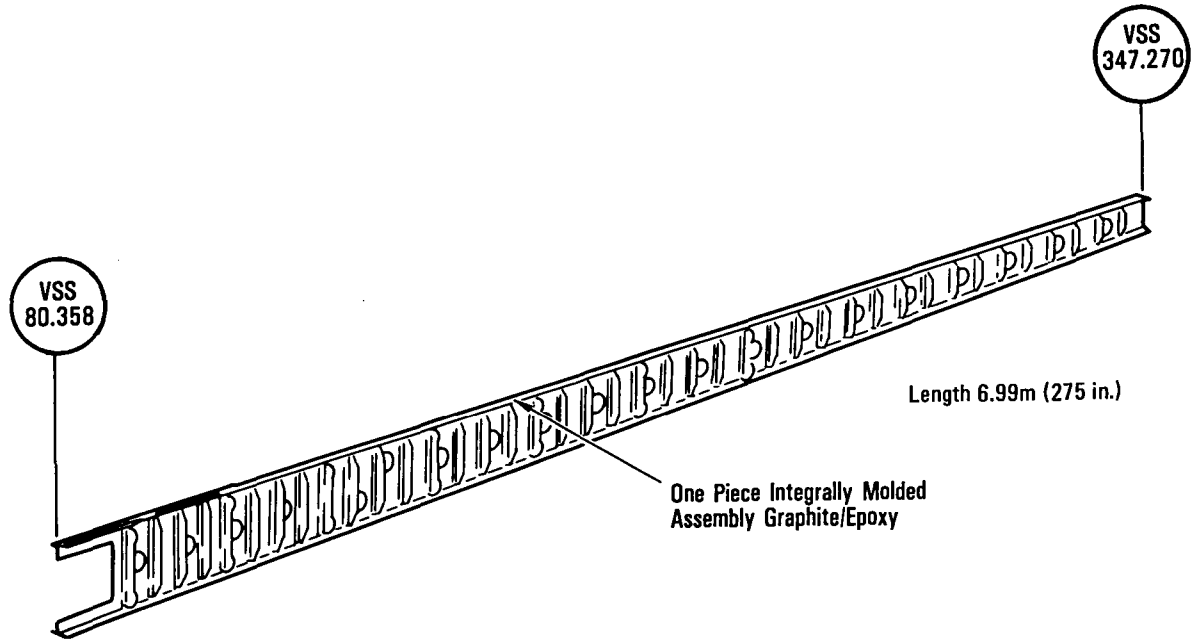

Figure 7. - Front spar assembly.

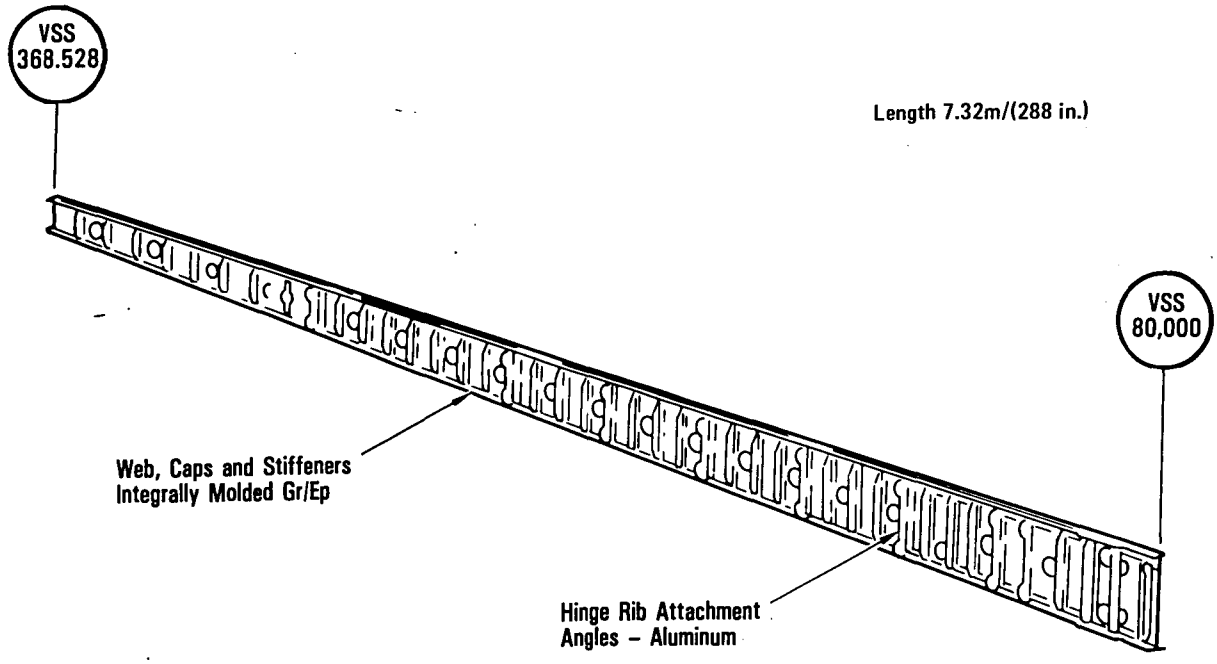

Figure 8. - Rear spar assembly.

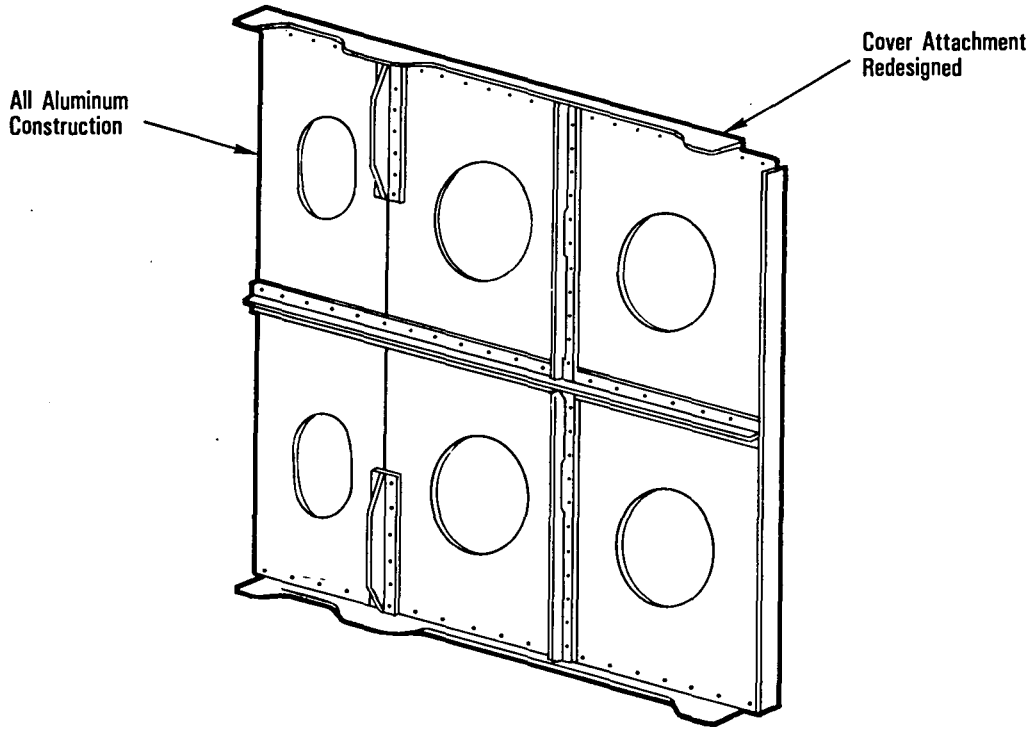

Figure 9. - Stub spar assembly.

suitably modified to accept the various advanced composite components. Use of this fixture (where rudder hinges, rudder actuator, and fuselage attachment control points have been retained) will ensure that all interchangeability requirements are met.

The fin box assembly is illustrated in Figure 10. Parts of the skin are cut away to show details of cover hats, ribs, and spars, used to assemble the L-1011 ACVF box. The fasteners selected for the assembly of major components are titanium hi-loks with stainless steel collars, which are wet-installed with sealant in close-tolerance, noninterference-fit holes.

Access to the inside of the box is accomplished by the removal of rib truss members and entry from the fuselage joint area. Limited hand access is also available through the holes provided in the front and rear spar webs. This access allows hi-loks to be installed at approximately 95 percent of all fastener locations and at the remainder, blind fasteners are used.

2. GROUND TEST HARDWARE

The ground test set-up is shown schematically in Figure 11. The fin box was mounted horizontally from a reaction frame with the right side down.

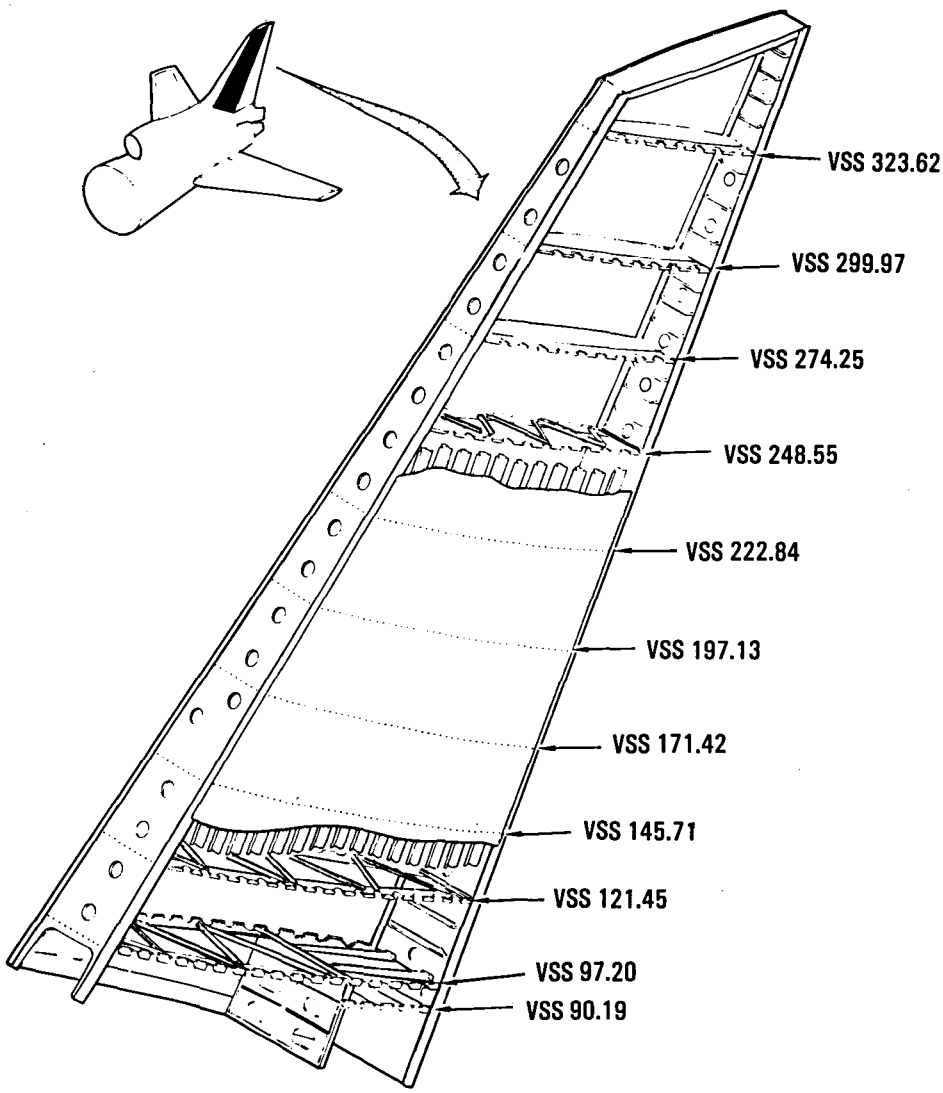

Figure 10. - Fin assembly.

2.1 Test Article Tie-Down

A transition structure was installed between the test article and the load reaction fixture. The purpose of this transition structure was twofold. Firstly, the fin-to-transition structure interface joint duplicated the actual joint mating the composite fin to the L-1011 aircraft. On the fin side of this joint, all structural members and attachment fasteners were installed per the aircraft assembly drawing configuration. Secondly, the transition structure induced the appropriate distribution of load within the fin as externally applied test loads were transmitted out of the fin and into the test fixture load reaction frame. The transition structure was attached to the reaction fixture with 'bath-tub' type fittings which were assembled around the periphery of the base. A photograph of this arrangement is presented in Figure 12.

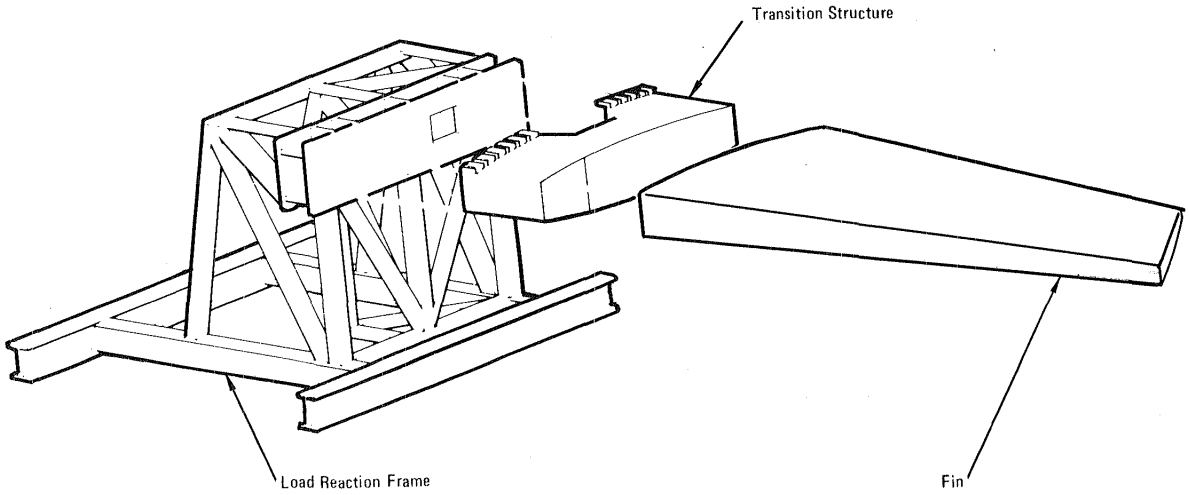

Figure 11. - Test installation of fin in load reaction frame.

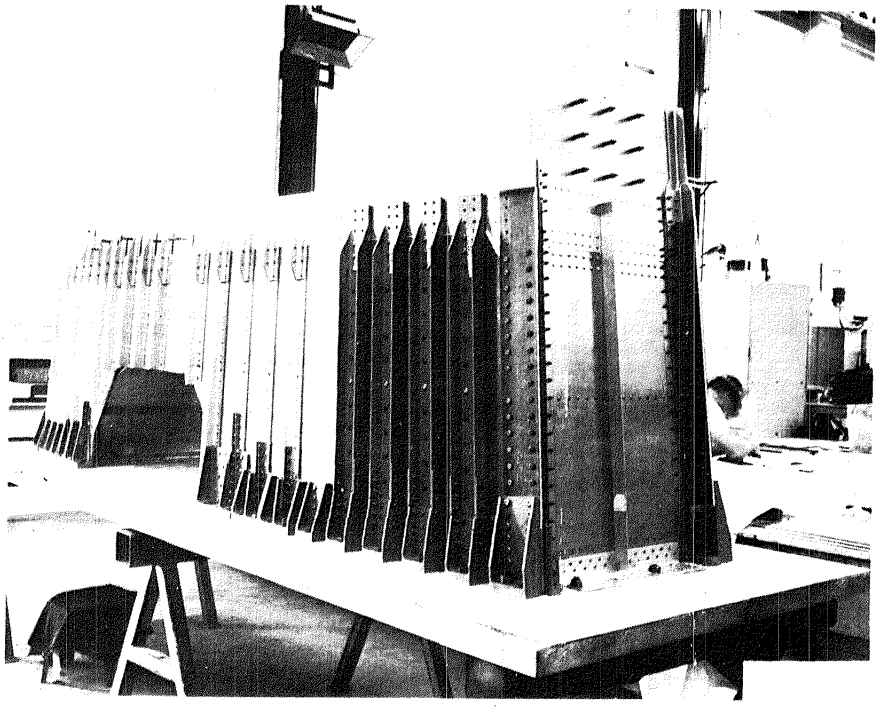

Figure 12. - ACVF - transition structure.

2.2 Test Article Loading Concept

The fin and transition structure were attached horizontally to the load reaction fixture with the right side facing down as shown in Figure 11. Externally applied side loads were introduced to the fin along the length of the front and rear spars from jack-trains which were mounted on the floor. Fore- and aft-direction external loads were applied to the fin through the

rudder actuator retention brackets at Vertical Stabilizer Station (VSS) 93.99. The jack-trains applying these longitudinal direction loads were installed parallel to the floor, in the same plane as the fin reference plane. They were cantilevered from a load reaction frame located aft of the fin rear spar.

2.2.1 Loading Attachments. - Eleven load fittings were attached to the front spar web at the following locations: VSS 97.2, 121.45, 145.71, 171.42, 197.13, 222.84, 248.55, 274.26, 299.97, 323.62 and 344.34. Five load proportioning beams connected adjacent fittings by pairs, grouped as follows: VSS 97.2 & 121.45, 145.71 & 171.42, 197.13 & 222.84, 248.55 & 274.26, 299.97 & 323.62. Test loads were applied to these five beams at the following locations: VSS 109.31, 158.56, 210.05, 261.40 and 311.80. A single fitting was loaded at VSS 344.34. Figure 13 illustrates a typical loading arrangement for the front spar.

A single load fitting was mounted on the rear spar web at location VSS 121.45. Side loads were applied to this fitting and also to the rudder hinge brackets at six locations: VSS 94.92, 146.79, 198.08, 249.36, 300.65 and 369.03. Figure 14 illustrates a typical loading arrangement for the rear spar.

Trunnion fittings were installed in the rudder actuator attachment fittings and jack-trains connected to both the left and right sides for application of fore and aft direction loadings.

Both the static and dynamic load tests employed a multi-channel, electro-hydraulic, closed loop system. Fifteen jack-trains were operated, controlled and monitored simultaneously. Dual bridge load cells, contained within each of the jack-trains, provided feedback signals to the servo controllers as well as signals for monitoring the loads.

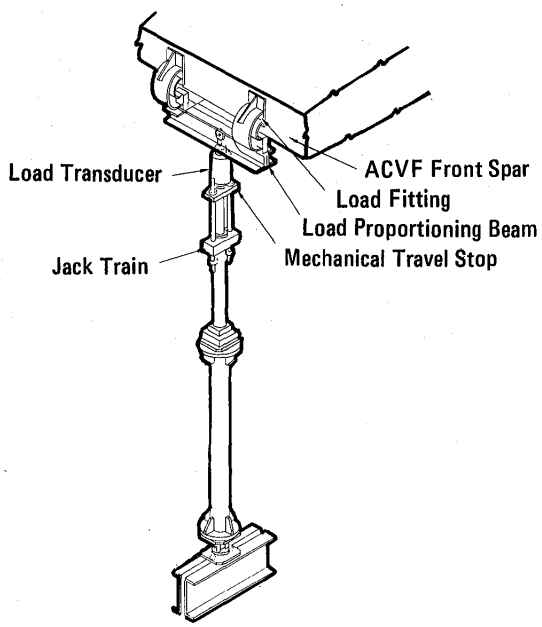

Figure 13. - Front spar typical loading arrangement.

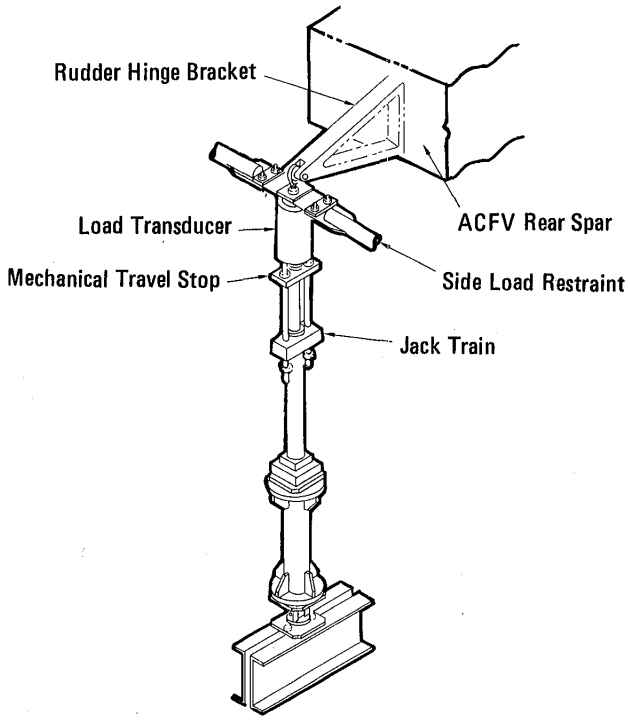

Figure 14. - Rear spar typical loading arrangement.

Hydraulic cylinders contained in the jack-trains generated the loads and were supplied from the laboratory hydraulic system which operates at a nominal pressure of 3000 psi.

Each of the fifteen jack-trains was equipped with a triple redundant overload protection system. Mechanical stops were provided in each train, and were backed off manually as load was applied, to the test article. The second protection system was achieved electrically by causing a system 'lock-up' and or hydraulic 'dump' when an error signal, required versus demand, exceeded a preset amount within the load control circuit. The third protection system provided pressure relief valves contained in the hydraulic networks which were preset to vent at 105 percent of the target pressure levels.

2.3 Test Set-up

Prior to mate of the advanced composite vertical fin box and the transition structure, the transition structure was fitted up to the reaction frame to check the alignment of the connecting holes as shown in Figure 15.

The fin and transition structure were than mated in a vertical position as shown in Figure 16. Some mismatches were found at the spar caps due to warpage of the splice angles during machining. The mismatches were shimmed and all joint holes pilot drilled from the inside out. The fin and transition structure were then separated and cleaned to remove dust from drilling. Faying surface sealant was applied and the two parts remated. The holes were

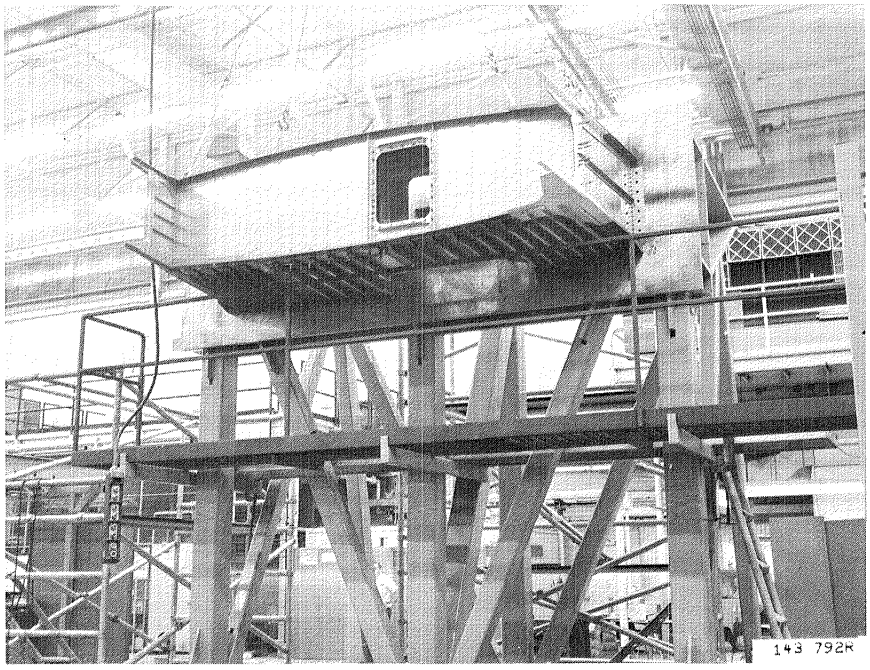

Figure 15. - Transition structure fitted to reaction frame.

then drilled to size and countersunk using a spacematic drill motor and carbide drills.

Upon completion of the mate, the assembly was attached to the reaction frame.

The setup and checkout of the ground test system was then accomplished. This included all jacks, load cells, linear variable deflection transducers, and strain gages. This part of the program proceeded well with only minor problems. The setup is shown in Figures 17 and 18.

Figure 17 shows the front spar loading setup. The front spar was reinforced between the two upper load fittings because of the high local load introduction. (See last paragraph Section 2.5).

Figure 18 shows the rear spar loading setup. All rear spar loads but one near the root were input through the rudder hinge fittings. The two horizontal jacks in the figure are used to apply the rudder actuator loads, primarily a couple, to the actuator support structure on the rear spar.

2.4 Instrumentation

Magnitudes of loads applied by the hydraulic cylinders were measured by a calibrated load transducer contained within each of the jack-train

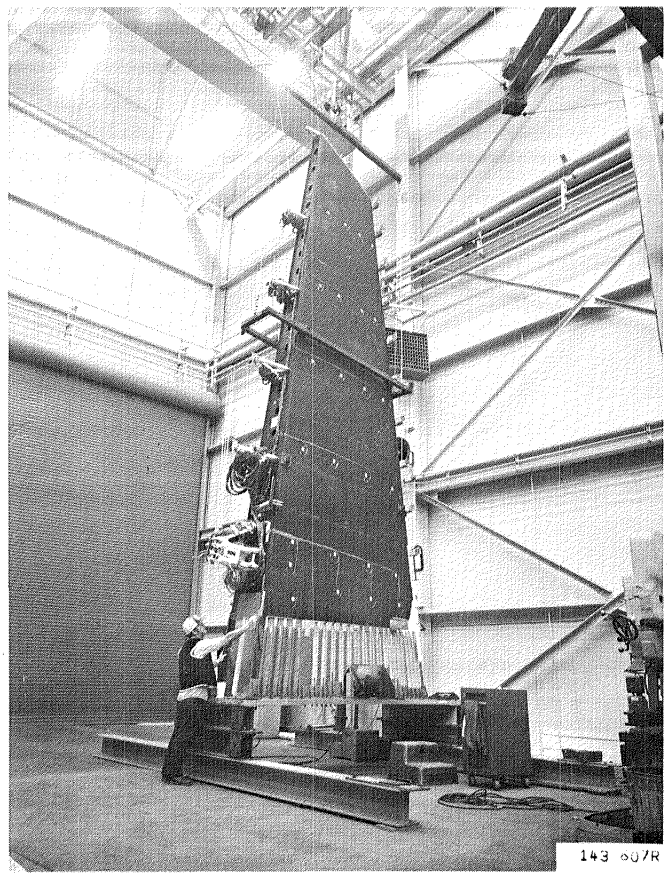

Figure 16. - Fin and transition structure mated.

assemblies. Nine linear deflection transducers were installed on the test article to measure displacements at the fin-transition structure interface joint, ribs VSS 97 and 197, and at the front and rear spar tips.

Strain gages were used to measure axial and shear strains at various locations on the fin. The strain gage locations are shown on Figures 19, 20, 21, 22 and 23.

Test parameters such as load magnitude, displacement and strain were input to a Central Data System (CDS) for recording and processing. Real time parameter history displays were available at the test site on a remote terminal cathode ray oscilloscope tube. Hard copy data sheets were available for inspection of content and analysis during the tests. The testing was filmed by high speed cameras.

2.5 Test Loads

The ground test article was tested to a high bending dynamic lateral gust case, Condition 59. This condition was critical for the front spar and covers and adequately loaded the whole structure. Graphic comparisons of 'desired' and 'test' shears and moments are presented in Figures 24, 25 and 26.

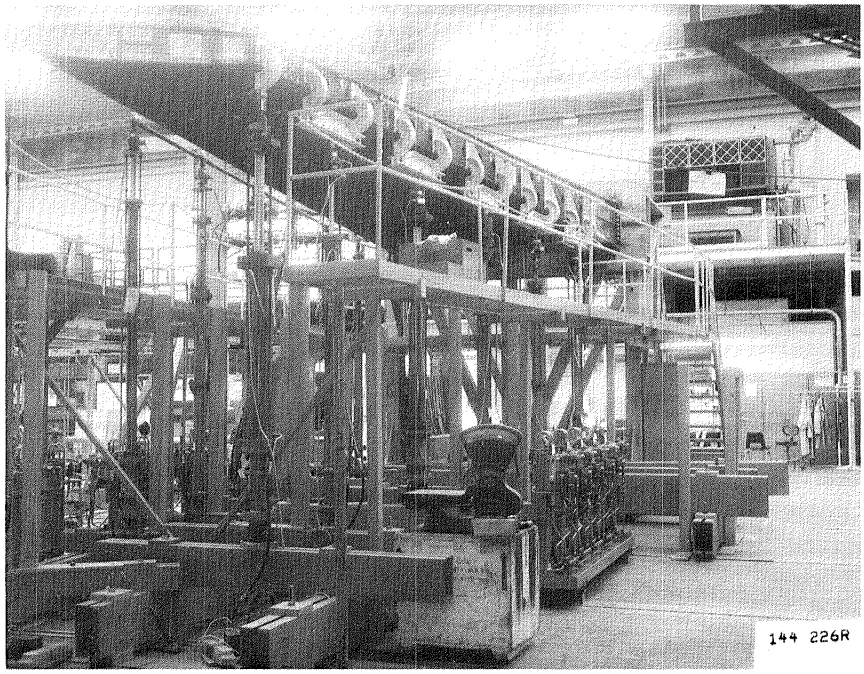

Figure 17. - Front spar loading setup.

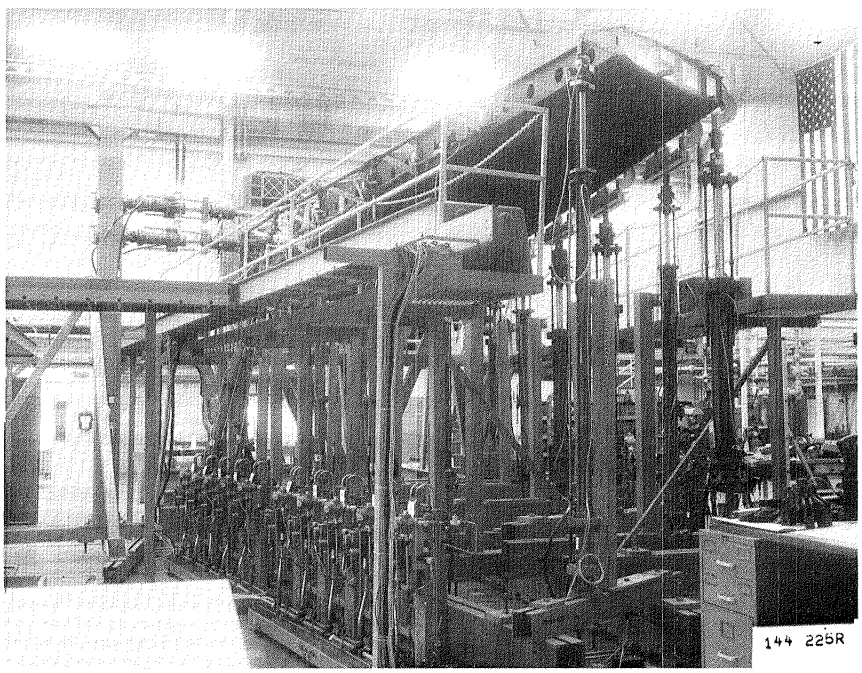

Figure 18. - Rear spar loading setup.

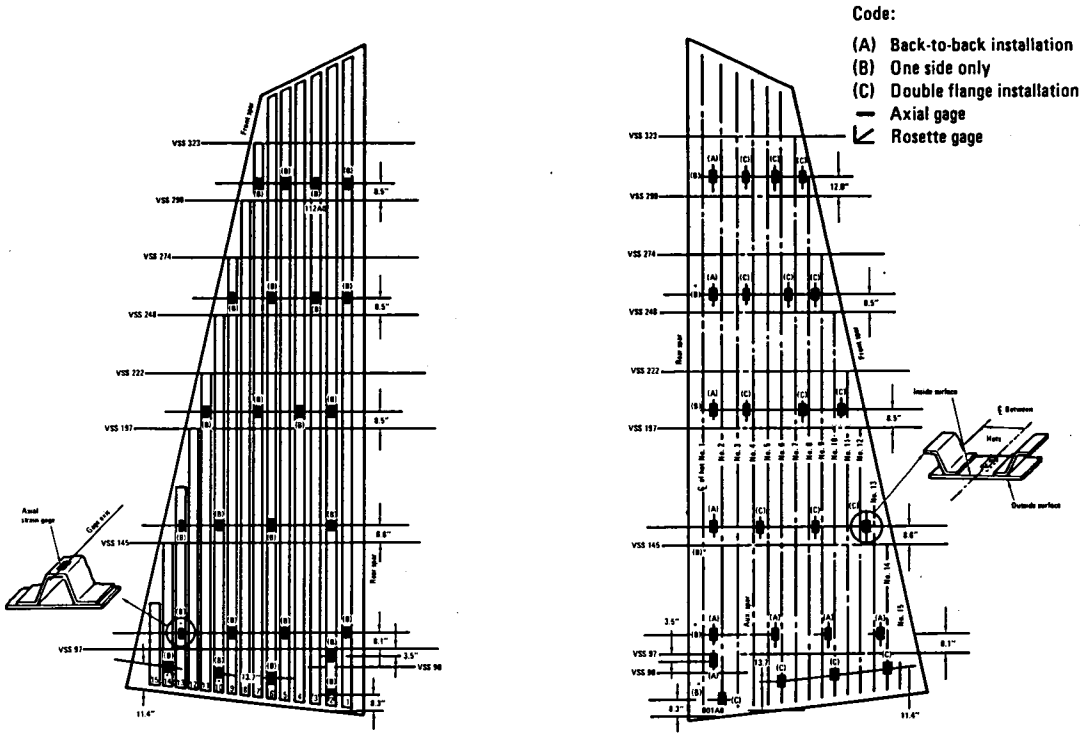

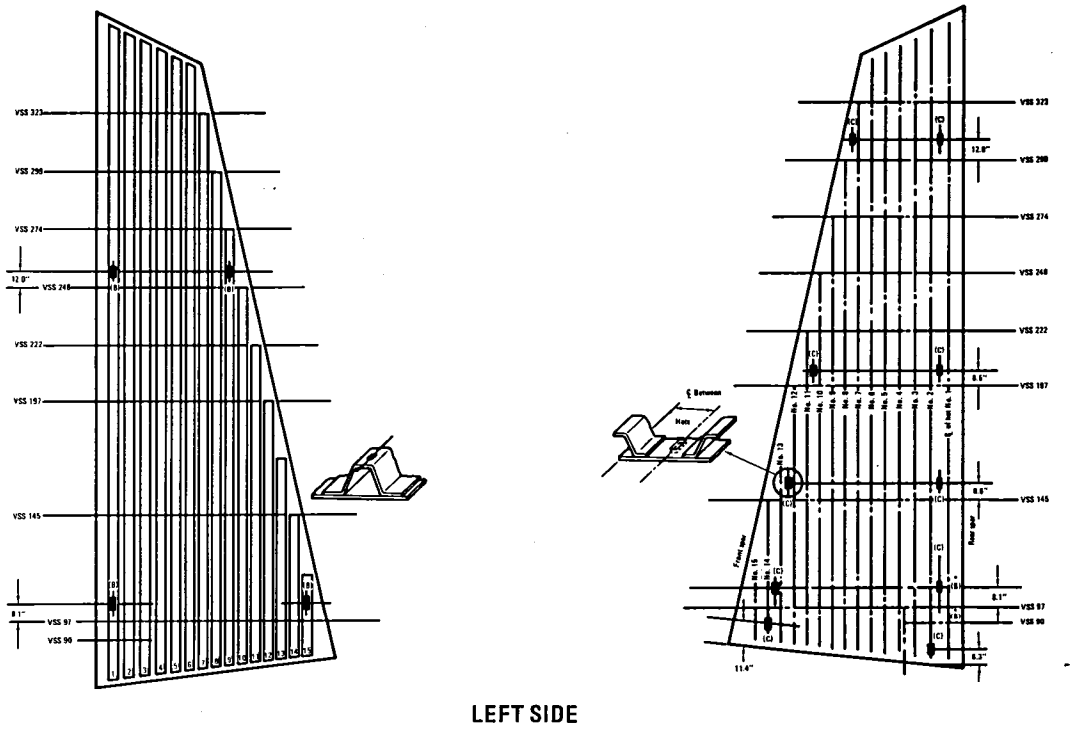

Figure 19. - Strain gage installation, right and left covers GTA No. 1.

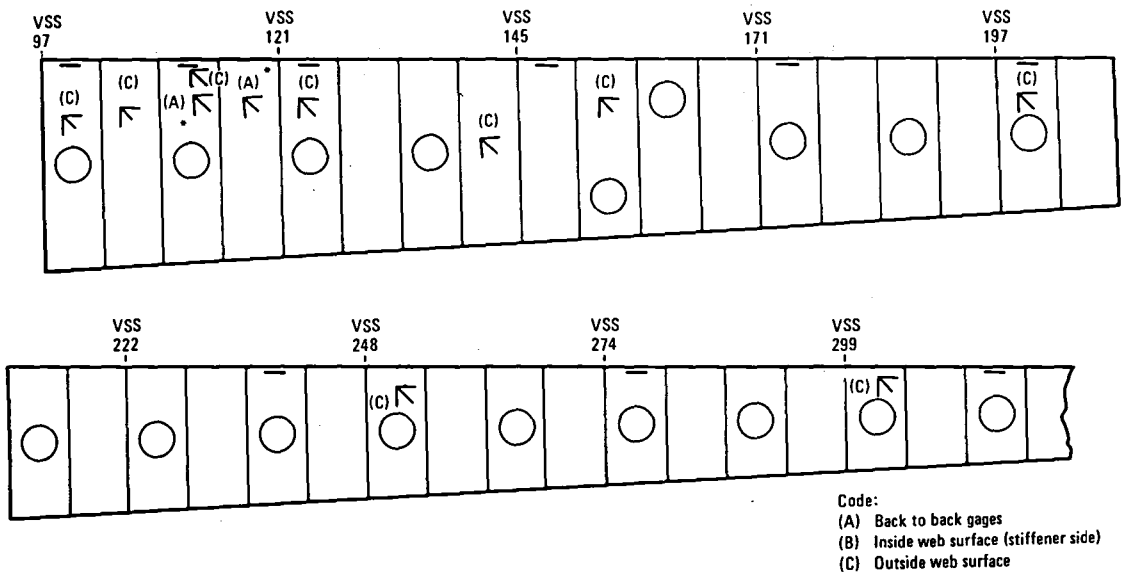

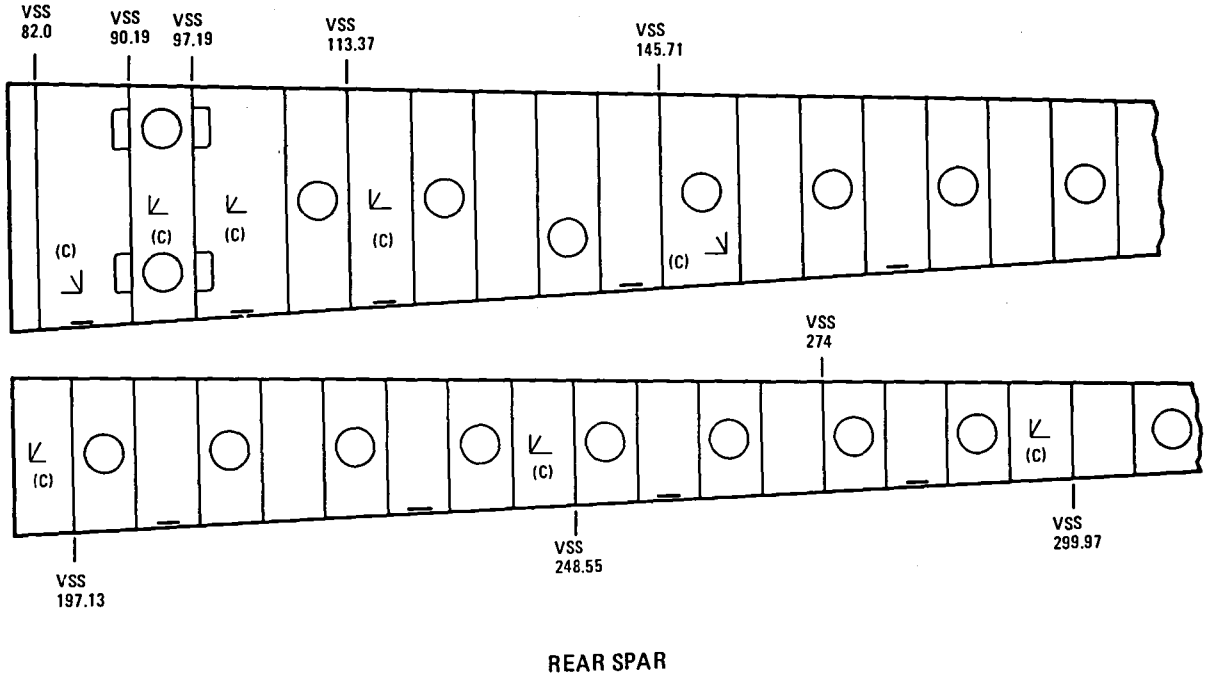

Figure 20. - Strain gage installation, front and rear spar GTA No. 1.

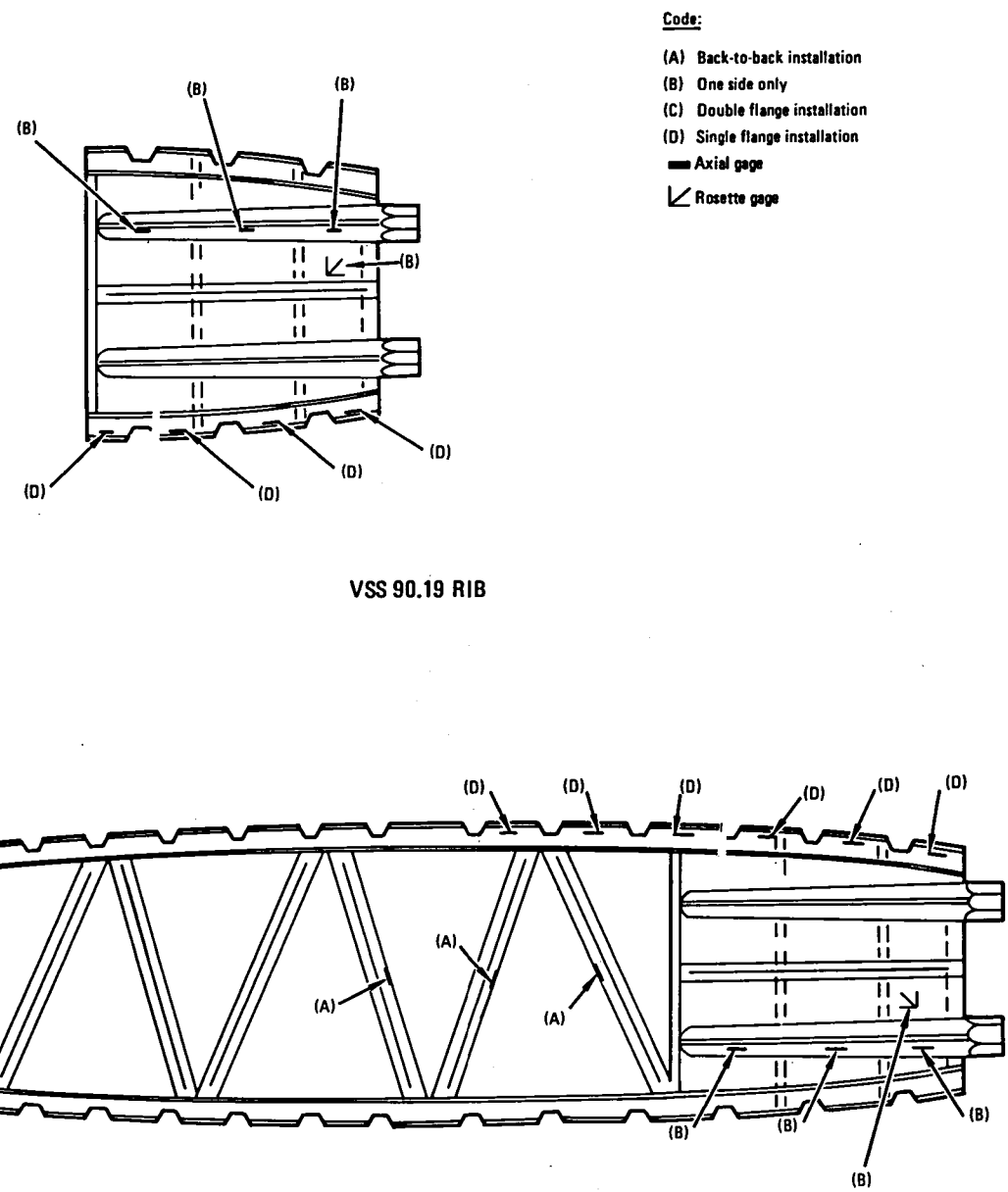

Figure 21. - Strain gage installation actuator ribs.

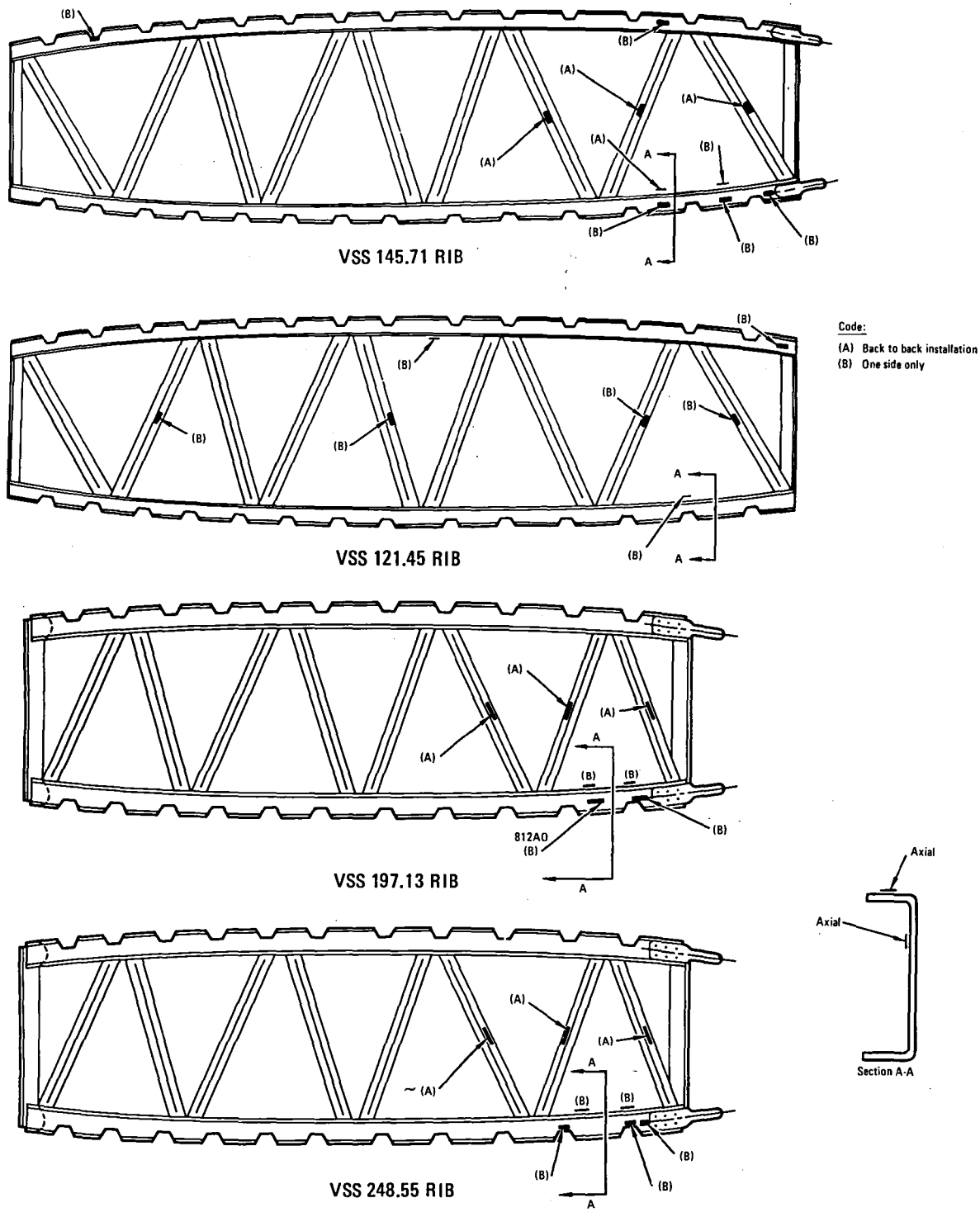

Figure 22. - Strain gage installation, truss ribs.

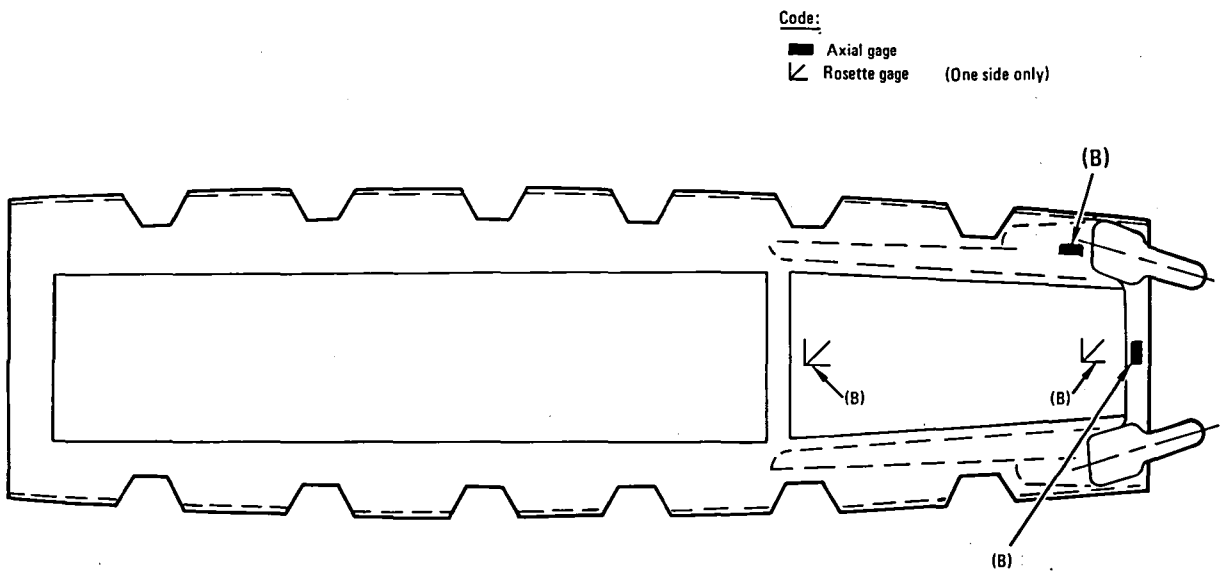

Figure 23. - Strain gage installation solid web rib.

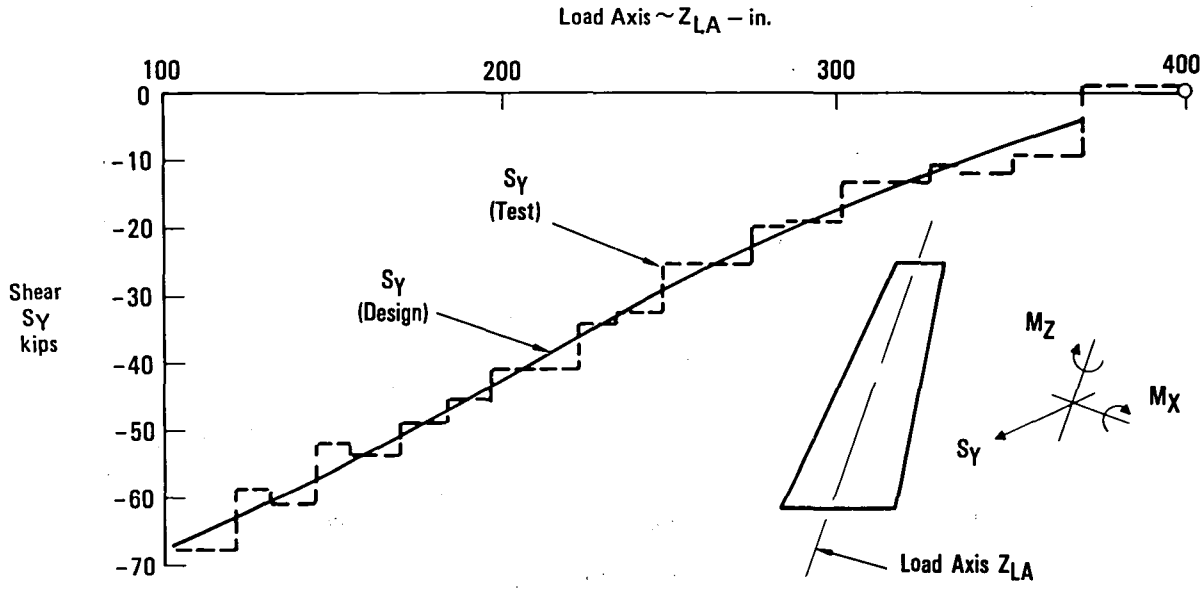

Figure 24. - Dynamic lateral gust condition 59 - shear S_Y.

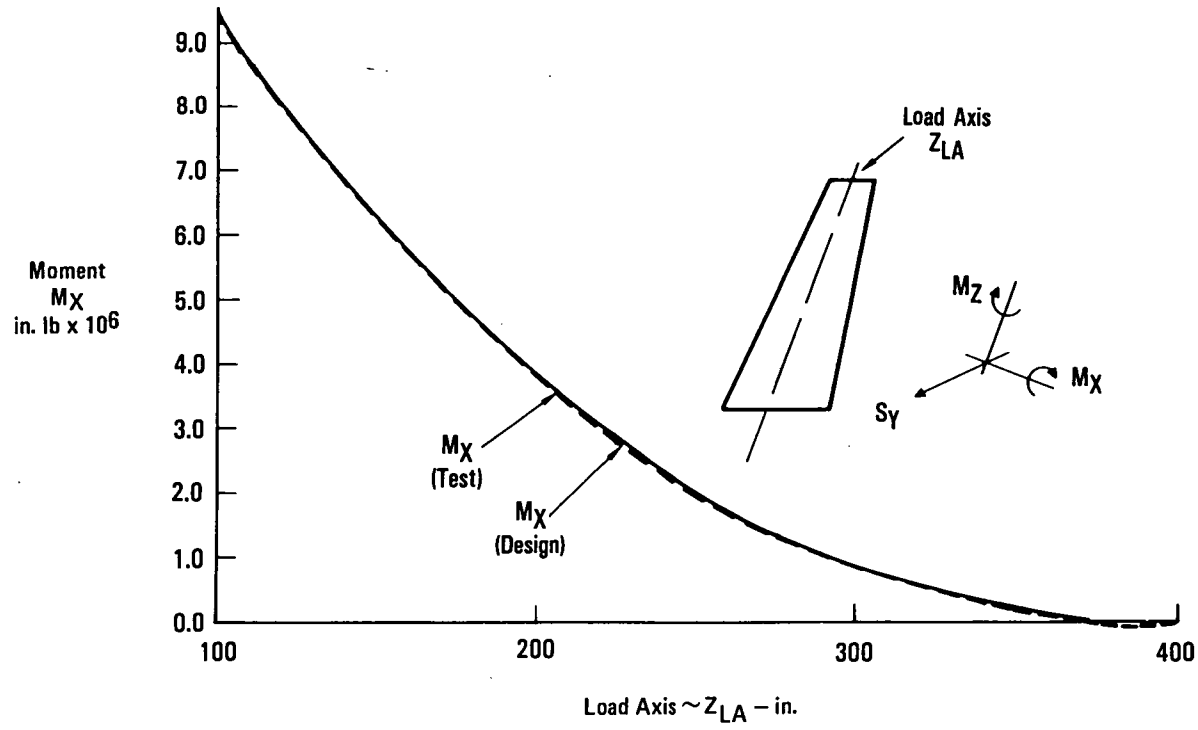

Figure 25. - Dynamic lateral gust condition 59 - bending moment - M_X.

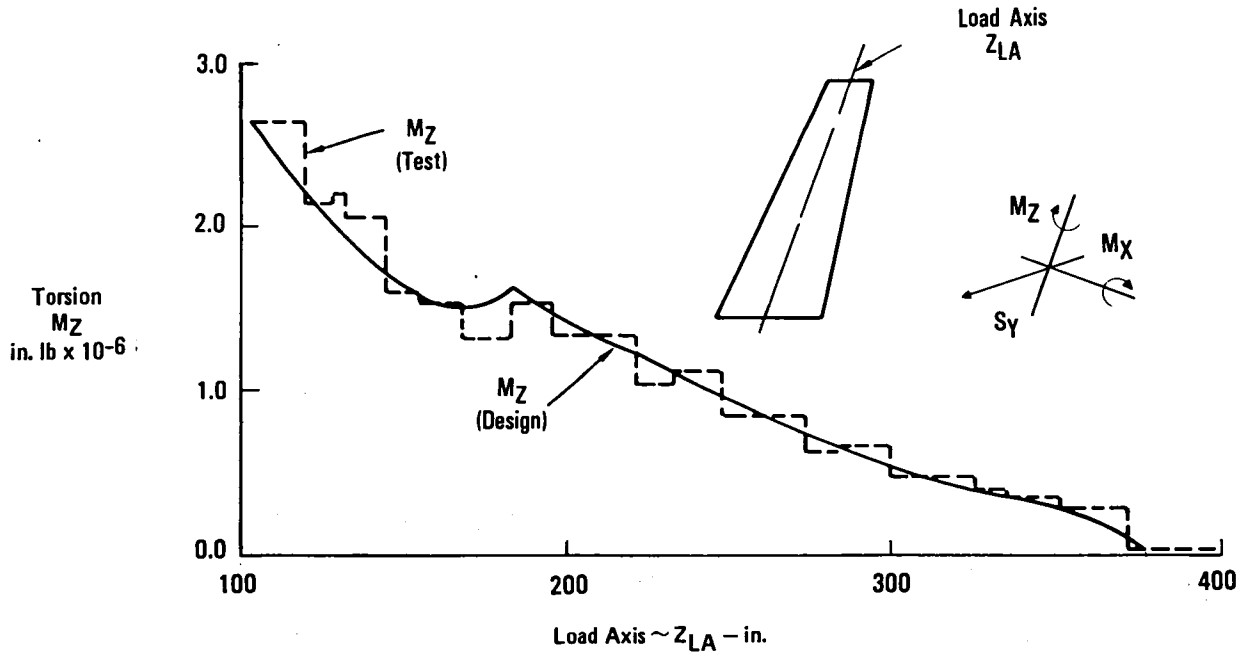

Figure 26. - Dynamic lateral gust condition 59 - torsional moment - M_Z.

Failure was anticipated to occur in the front spar web and be preceded by buckling. Those buckles would cause a buildup of interlaminar tension between the web and stiffeners to the point of separation. The room temperature dry failure was predicted to occur at 136 percent DUL.

A series of tests were run to find the effect of environment on hat and tee stiffener pull-off loads. At R.T. Dry the average tee pull-off load for a two-inch long tee was 483 lb, and at 180°F wet was 401 lb. Until buckling is initiated, there is no interlaminar tension force acting between the stiffener and the web. Once buckling is initiated, interlaminar tension loads are assumed to increase in a linear fashion until failure. Data from coupon tests performed during Phase II showed that compression and shear modulus at 180°F wet is generally as high as or higher than that at room temperature (R.T.) dry. Thus, buckling initiation was not expected to be reduced at 180°F, wet, compared to R.T., dry. Figure 27 shows a plot of the interlaminar tension force versus percent of design ultimate load showing zero interlaminar tension at 96 percent DUL and 483 lb at 136 percent DUL. Interpolating for 401 lb gives a predicted failure at 180°F wet of 129 percent DUL. Thus, the environmental factor applied to Condition 59 was 136/129 = 1.06.

A NASTRAN model of the composite fin including the transition structure was run and the resulting internal loads were compared with those from the NASTRAN model of the composite fin coupled to the L-1011 with flight loading. The resulting comparison is shown in Figure 28. Because of the high applied loading in the front spar web near the tip, a special test reinforcement was applied.

3. STATIC GROUND TEST

Two static ground tests were performed. The first resulted in an unexpected failure at 98% DUL. Following an investigation into the cause of the failure GTA No. 2 was reinforced and the test program continued.

3.1 Ground Test Article No. 1

An investigation was initiated to find the cause of the premature failure. The results are described below, along with the test history.

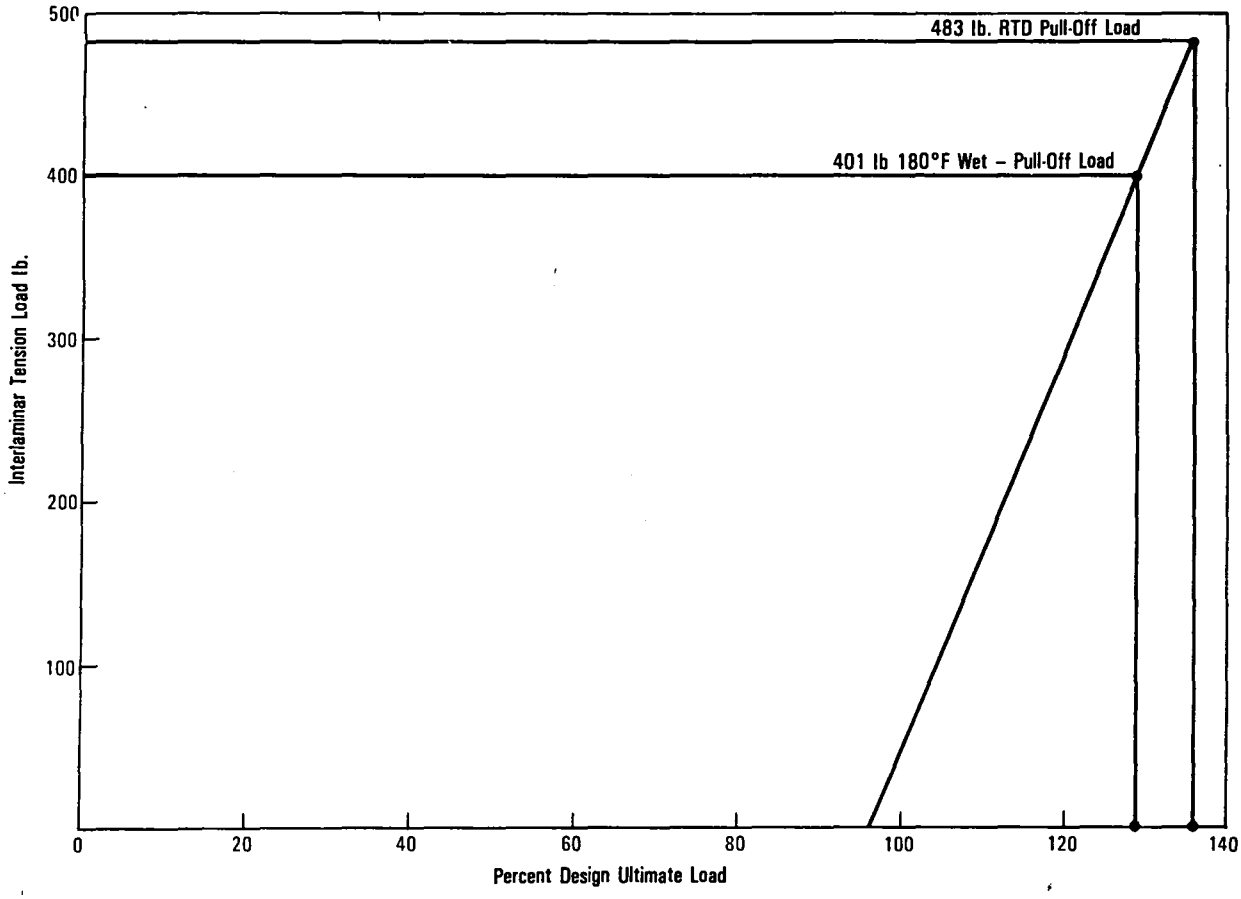

Figure 27. - Interlaminar tension loads versus percent DUL.

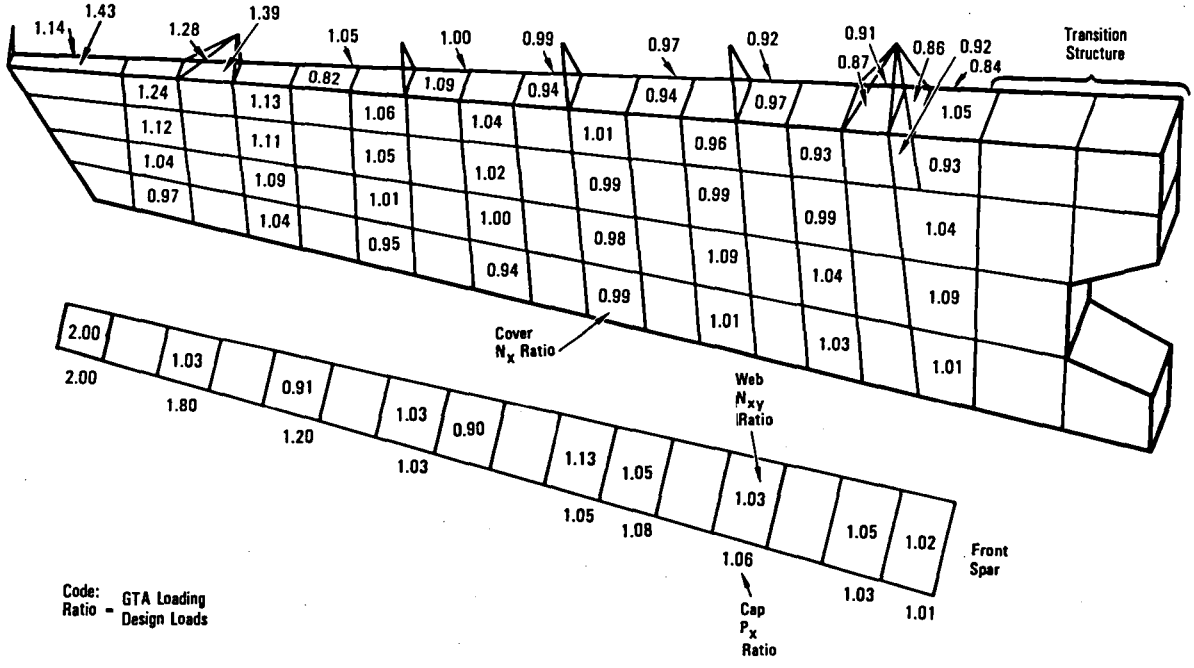

Figure 28. - Internal loads comparison.

3.1.1 Test History.-During one of the pretest strain surveys, close examination revealed a buckle developing in the edge of one of the access holes in the lower portion of the front spar at about 30 percent DUL, although no buckling was detected by strain gages away from the hole up to limit load. Based on prior subcomponent tests, no buckling had been anticipated at a hole edge below limit load and no buckling away from the edge below ultimate load. As the spar had not been designed for diagonal tension loads, it was decided to stabilize the lower six access holes by clamping the edges between two aluminum rings to prevent the web from buckling. The installed rings are shown in Figure 29. Ground testing was initiated on May 14, 1981. The fin box was first loaded to Design Limit Load (DLL), or 2/3 DUL for Condition No. 59. A review of selected quick-look data channels showed that the fin box was performing as predicted. While the data were being reviewed the loading was reduced to 10 percent and held. This was standard procedure throughout the test.

The test loading was next increased to 80 percent DUL at which point loud popping and cracking sounds were heard. The load was reduced and a visual inspection performed. It was found that some blind fasteners (MS 21140-06) in the left hand fron spar cap-to-cover joint had tipped. The use of blind fasteners is restricted by the fin assembly drawing to the left had cover-to-solid web rib cap connection. These ribs prevent the necessary access to install the HL 13 pins and HL 94LP collars. The reason for installation of blind fasteners in the upper portions of the front and rear spar cap-to-cover connection from VS 222 on the left hand side was stated on a discrepancy report to be mechanic error. No corrective action was taken

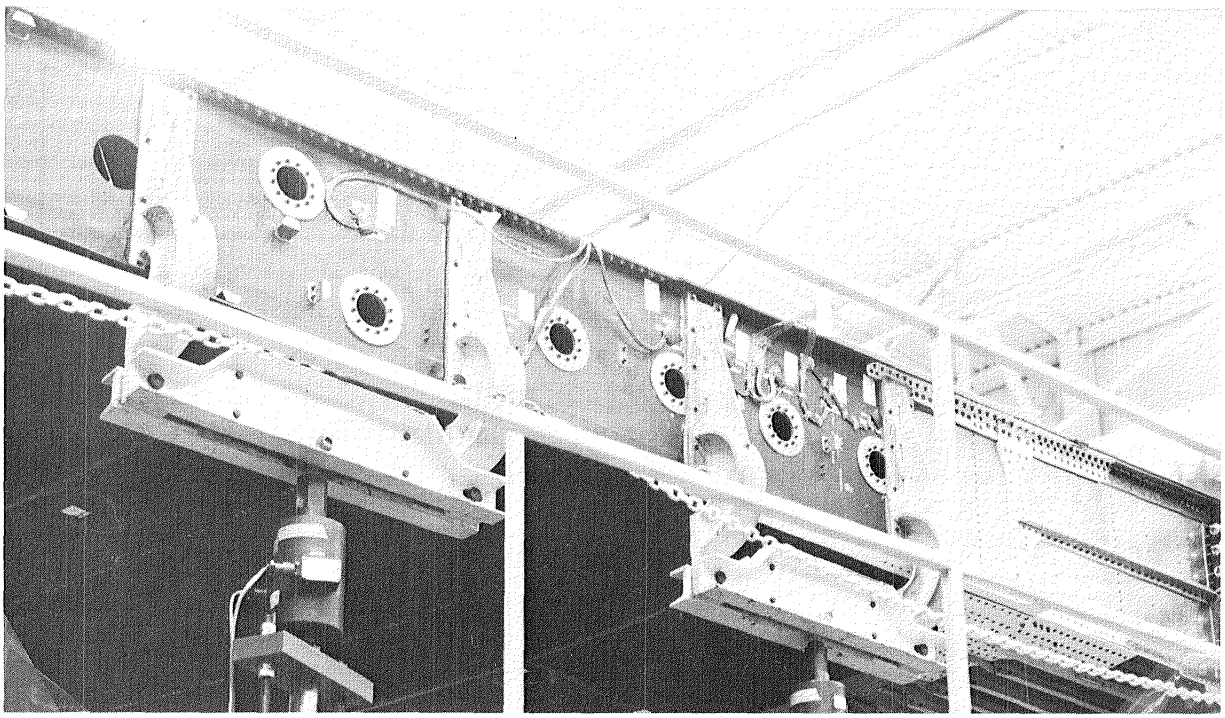

Figure 29. - Front spar web access hole reinforcement.

to remove these fasteners as their strength was judged to be sufficient to provide a positive margin in this location. The blind fasteners in the front spar and 78 of the more highly loaded blind fasteners in the rear spar were removed and replaced with 1/4 inch or 3/16 oversize Hi-Loks. The 1/4 inch fasteners were installed in holes which had been damaged by the tipping and could not be cleaned up at the 3/16 oversize. The heads on the 1/4 inch Hi-Loks were shaved for 0.08 countersink depth, the same as the 3/16 inch diameter. Figure 30 shows the areas where the fasteners were replaced.

The testing was resumed on June 11, 1981 after completion of the fastener replacement. The sequence of events was as follows:

- After completion of the system checkout, the load level was raised to 10 percent of DUL. The applied loads were checked to ensure that the system was operating properly.

- The load level was then increased to DLL and the quick-look data channels were reviewed and checked against predicted and previous test strains. This check showed that the box was behaving as anticipated. A visual examination of the exterior surface of GTA No. 1 showed no damage.

- The load level was then raised to 90 percent DUL. Some creaking noises were heard between 80 and 90 percent. Strain measurements compared well with anticipated results.

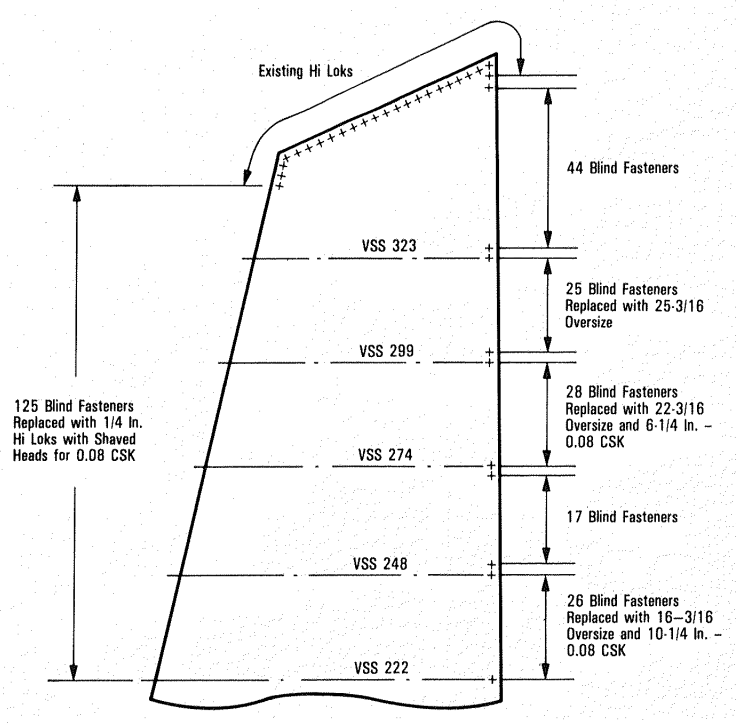

Figure 30. - Fastener replacement.

- The load level was next raised toward the goal of 106 percent DUL. At 98 percent DUL failure occurred.

3.1.2 Failure Investigation.-The failure resulted in damage to the front spar left hand cap from root to tip, local left hand cover damage including separation of the skin and stiffener in the runout bays toward the tip, separation of rib to front spar web attach members at all rib stations, and left hand rib cap damage on most of the truss ribs along the line of a skin buckle between cover stiffeners eight and nine. The left hand cover was the tension surface in this test.

The failed fin box is shown in figure 31 and figure 32 shows the locations of the failures. Examination of movie film taken during the test indicated that failure initiated in the front spar cap between VSS 299.97 and VSS 323.62. Six frames of the movie film are shown on Figure 33 and indicate the failure sequence. These frames were computer enhanced by J.P.L. to improve their clarity. Figures 34 and 35 show the primary failure zone.

The rubber mat laying on top of the test article shows a dynamic response to the fin failure. The wave mode bears no direct relationship to the failure mode.

The failure sequence has been identified as follows: The spar cap failed first in interlamina tension between VSS 299.97 and VSS 323.62. The failure then progressed along the spar to tip and then to the root. The initial failure and subsequent progression along the spar caused an increase in axial load in the free edge of the cover and high torsional deflections resulting in tearing of the cover at solid rib stations VS 299.97 and VSS 274.25, buckling of the skin and disbonding of hat stiffeners near the front spar. Figure 34 shows the skin tear at VSS 299.97. Due to the open box section the shear center shifted aft behind the rear spar and caused a large increase in the compression load in the left hand truss rib caps resulting in progressive failure of the rib caps down to and including VSS 145.71. Figure 36 shows the rib cap failure at VSS 248.55. This is typical of the rib cap failures. The rotation of the spar cap about the right hand surface (lower surface in test set-up) caused failure of the rib connection to the spar.

A review of the design details uncovered a deficiency in the spar design. The front spar cap and web-to-cap configuration in the area of the primary failure is shown in Figure 37. This portion of the cap consists of four plies of $+45^{o}$ or -45^{o} orientation, then ten plies of 0^{o} orientation, and four more $+45^{o}$ or -45^{o} plies. The four plies from each side of the spar web are continued around to become part of the spar cap. The remaining twelve plies terminate at the cap. A photomicrograph (Figure 38) of a section of the right hand spar cap, with a similar configuration to the left hand cap in the primary failure zone, shows that failure has initiated in this location. The four plies of web material are separated from 0^{o} cap material through the radius and into the flange. A crack extends across the web. A microcrack is also visible in the spar cap. By contrast Figure 39 shows a photomicrograph of a comparable section taken from an untested spar cap. No cracks are visible in this section.

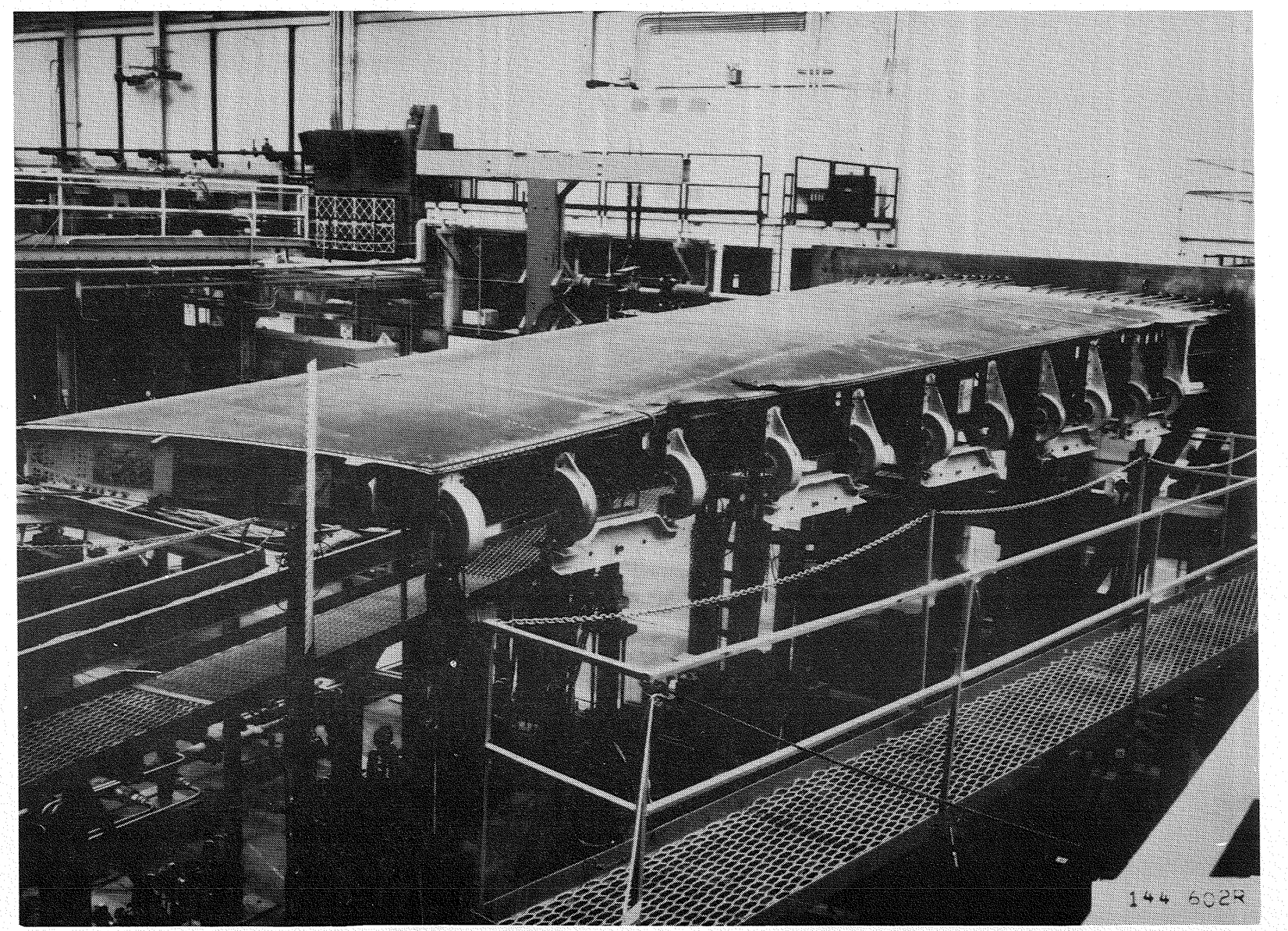

Figure 31. - Test component after failure.

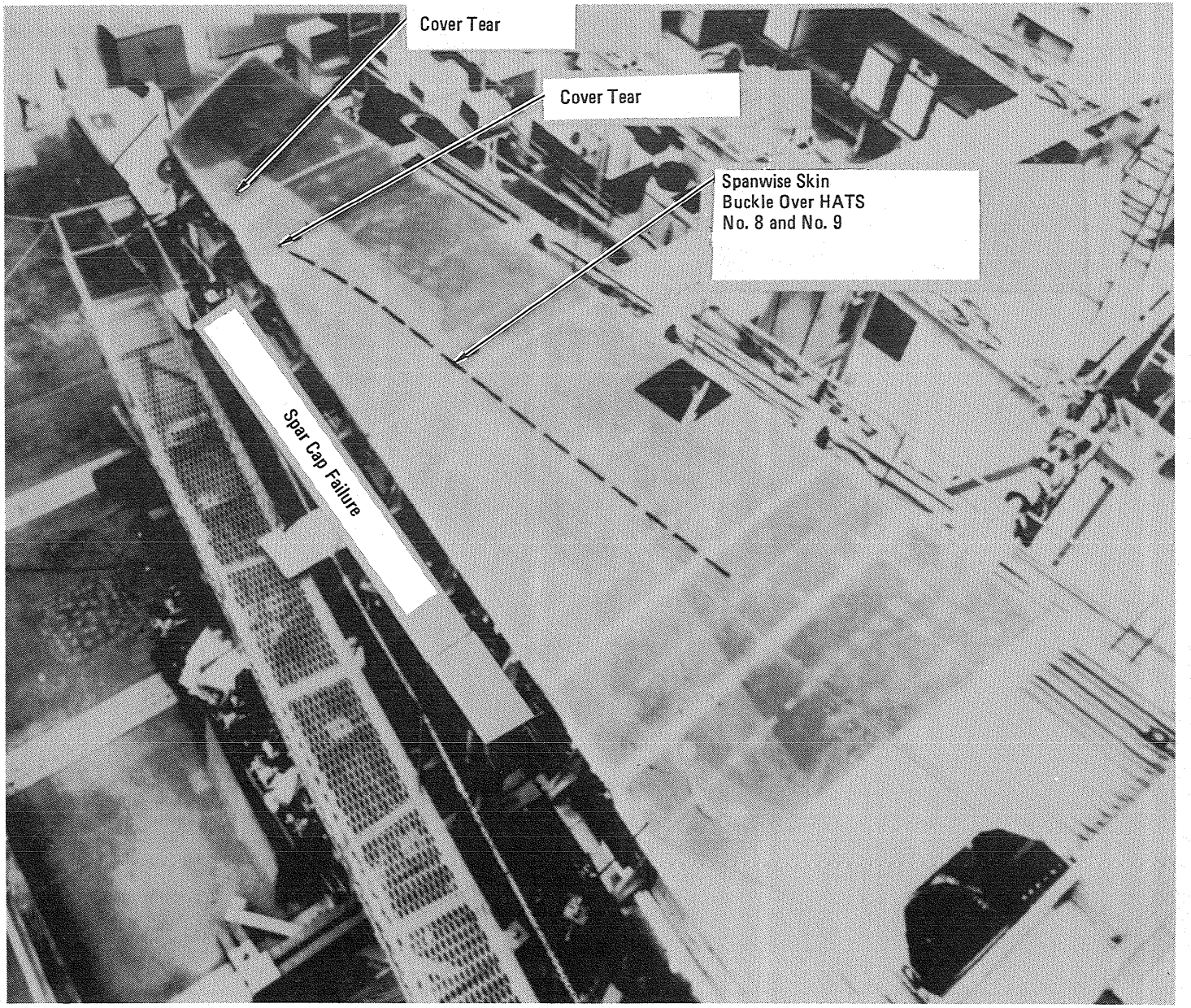

Figure 32. - Overall view of failure.

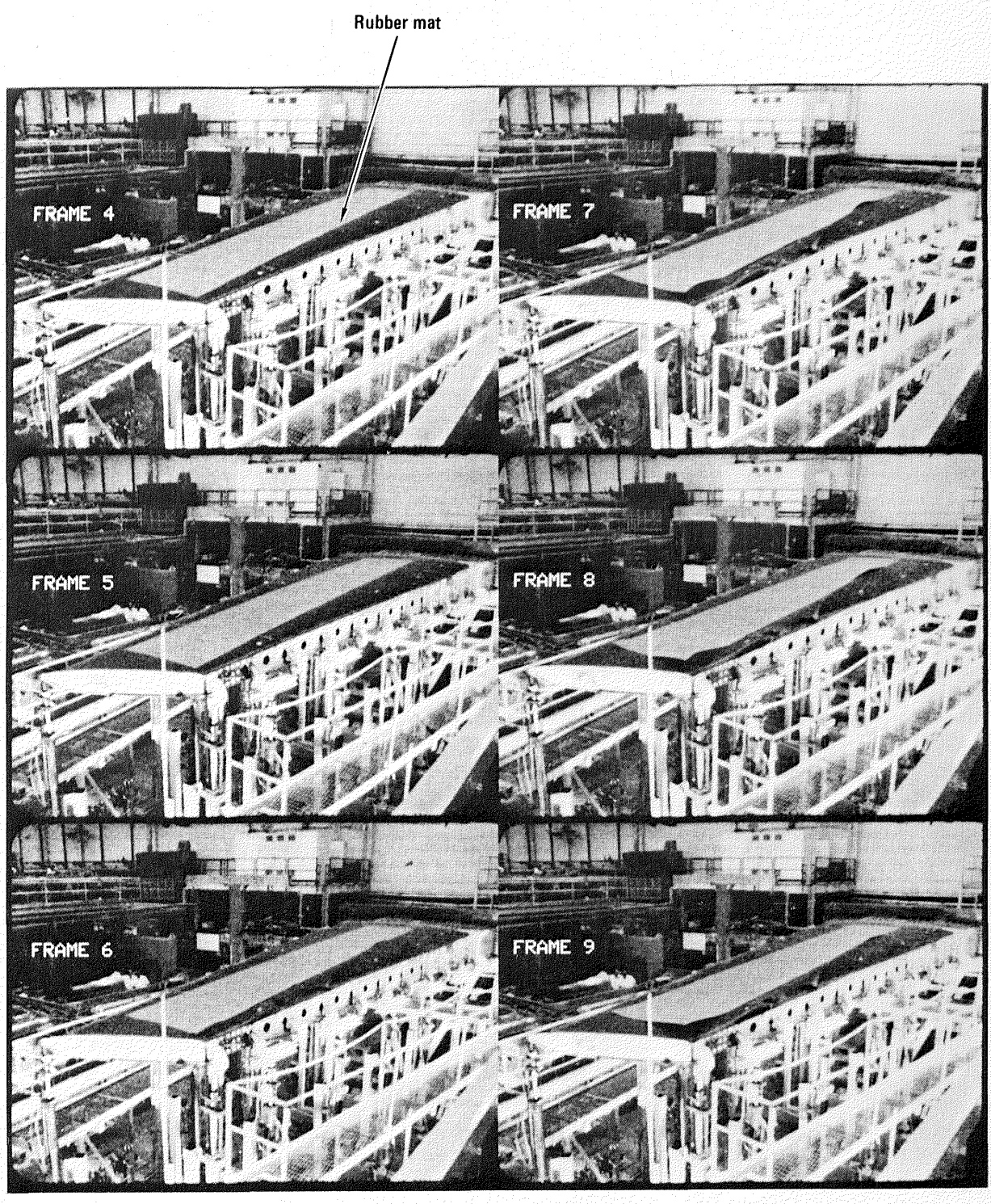

Figure 33. - Six frames from high speed movie showing failure sequence.

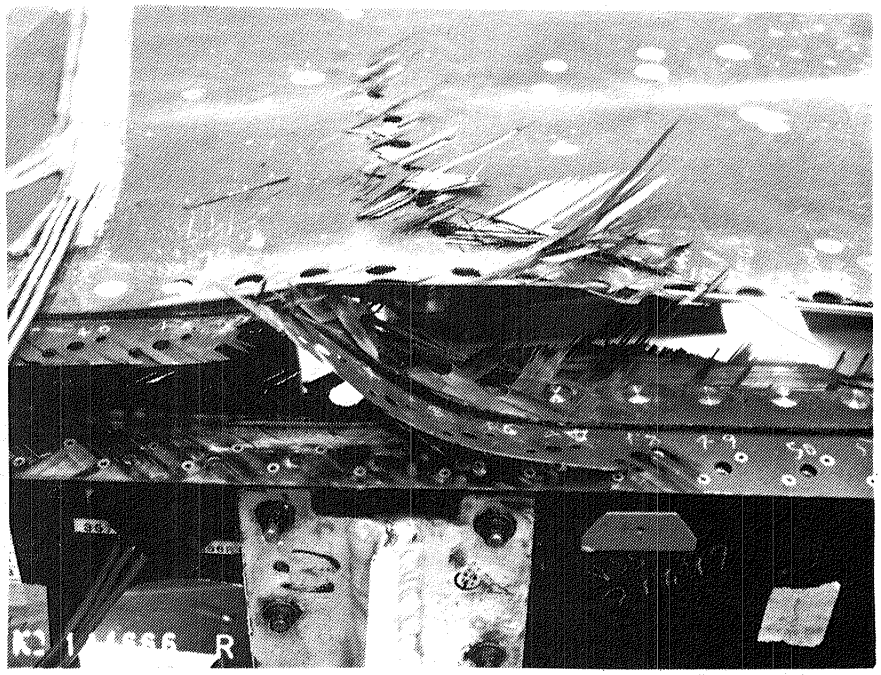

Figure 34. - View of failure at VSS 299.

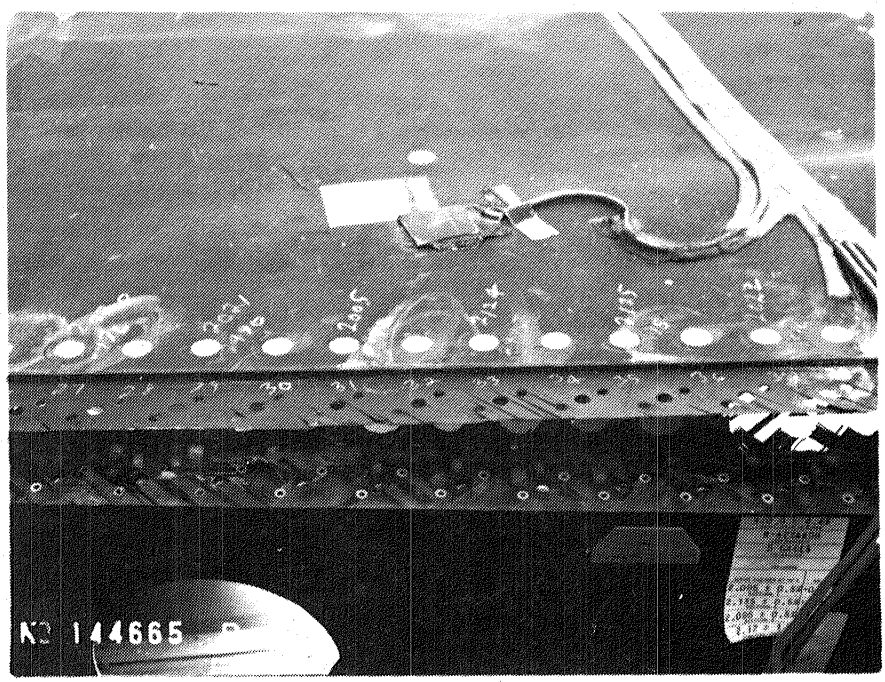

Figure 35. - View of failure at VSS 307.

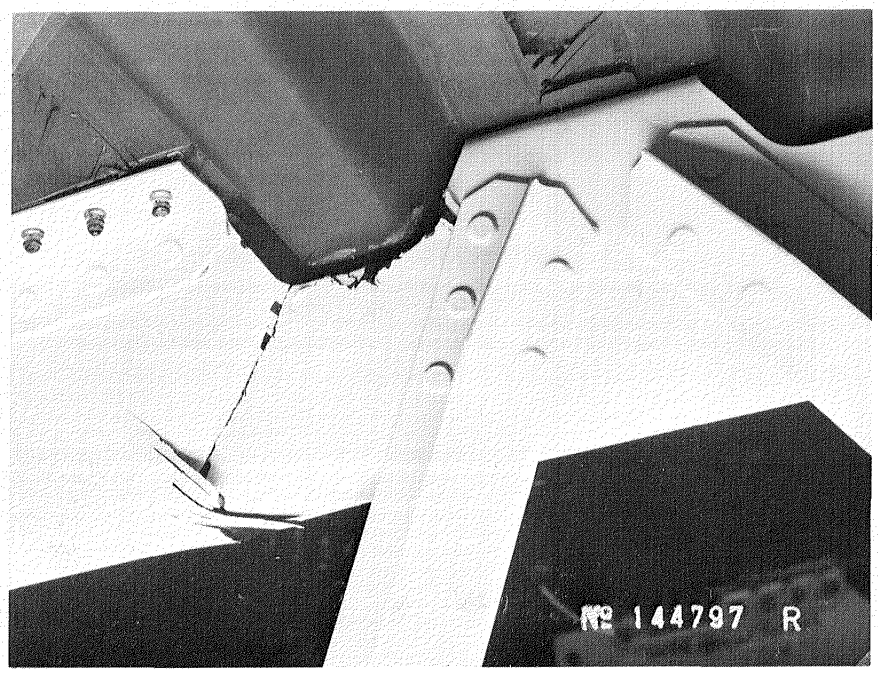

Figure 36. - Typical rib cap failure

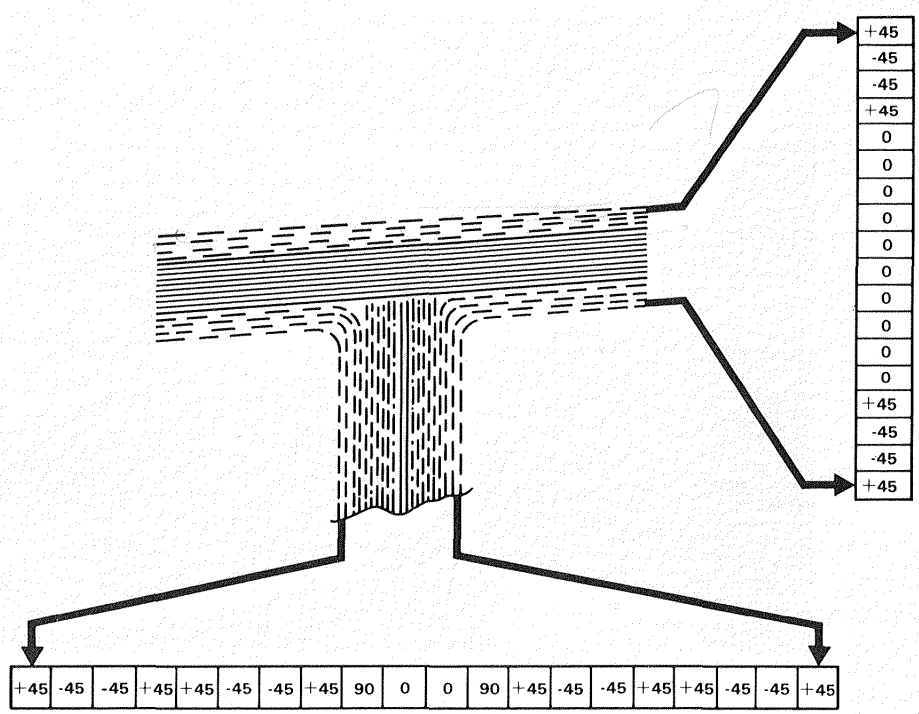

Figure 37. - Front spar cap configuration in primary failure zone.

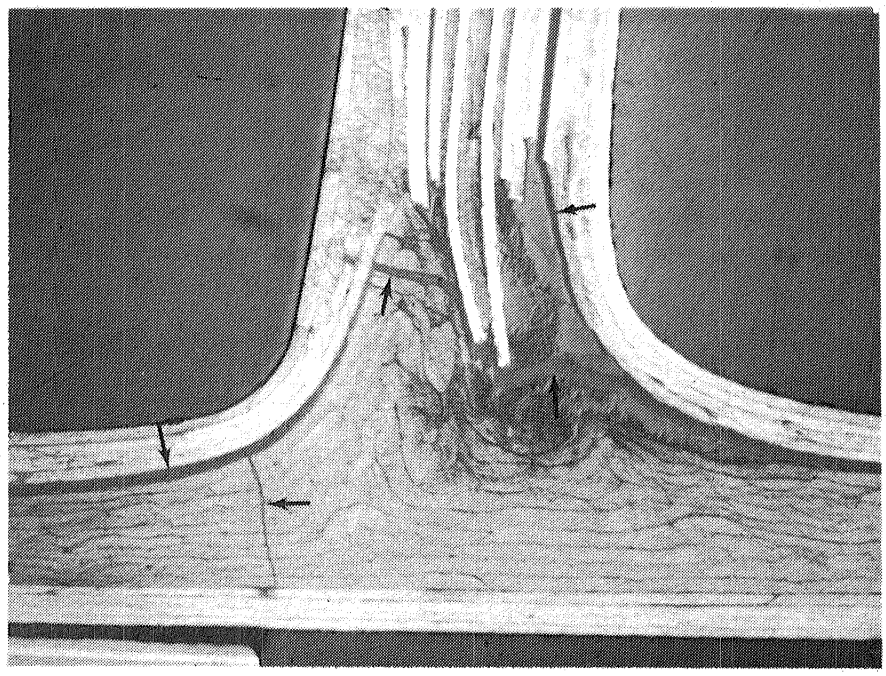

Figure 38. - Photomicrograph of section from GTA No. 1 front spar cap, right side at VSS 277.4.

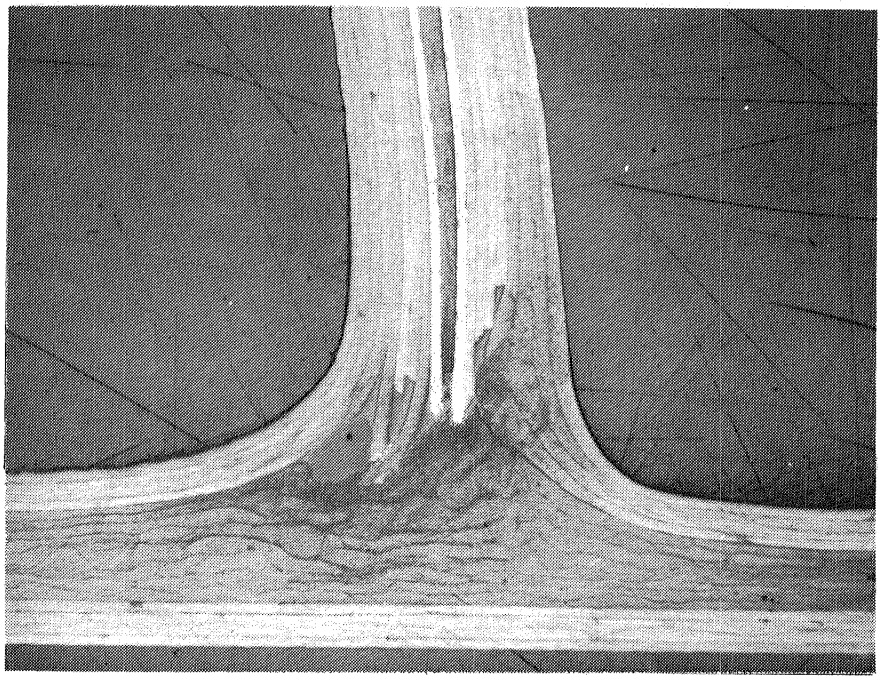

Figure 39. - Photomicrograph of section from untested spar cap.

A redesign of the spar includes taking all the web plies around into the cap and the cap would be designed for a minimum out of plane loading.

The out of plane loads come from several sources but in particular from the shear buckling of the cover in the bay adjacent to the front spar cap.

The damage in the primary failure zone is shown pictorially in Figure 40. Failure consisted of separation of the $\pm 45^{o}$ plies from the 0^{o} plies with the failure propagating from one interface to the other through the 0^{o} plies. The failure was caused by out-of-plane loads which inflicted interlamina tension and bending on the spar caps. These loads come from several sources. Transverse cover loads are due primarily to Poissons effects and are offset from the spar cap mid plane, thus introducing bending. Shear buckling of the trapezoidal panels adjacent to the front spar cap (see Figure 41) introduce both bending and normal loads to the spar cap plus diagonal tension loads. A load will also occur from the spars pulling down the upper cover to conform with the deflected shape. The cover curvature due to airfoil camber also introduces a normal component of load. Some of the loads are additive and some subtract and the net effects will vary with location.

A series of tests was run to duplicate the failure modes of the spar cap and the rib caps. A visual and pulse echo inspection of the right hand cap of the front spar did not indicate any damage. Segments were cut from this cap for interlamina tension, transverse tension and in-plane shear tests. Sections were also cut for micro-analysis. The micro-analysis showed that damage had indeed occurred in the spar cap as shown in Figure 38. Tests were thus also performed on segments cut from the same zone of a virgin front spar which had never been assembled into a box or subjected to any loads. One

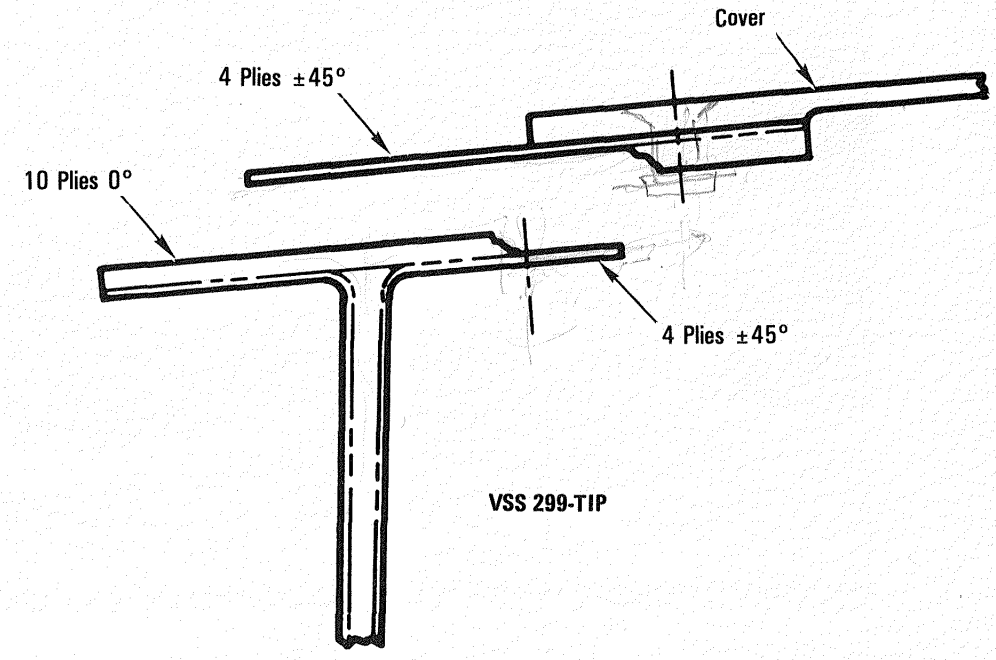

Figure 40. - Diagramatic view of primary failure.

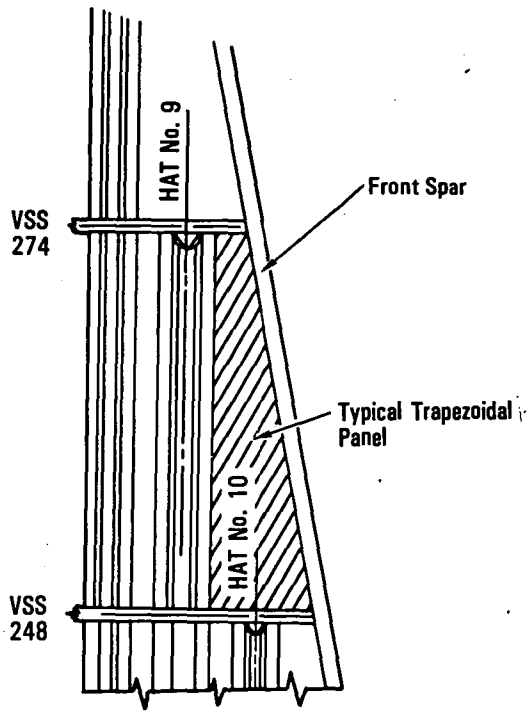

Figure 41. - Location of typical skin trapezoidal panel.

specimen each for interlamina tension test and transverse tension test from this virgin spar was subjected to a low cycle high-load fatigue spectrum representative of the strain surveys and tests performed on GTA No. 1 prior to the test which resulted in failure.

The results of the interlamina tension tests on the spar caps are shown in Table 1. The specimen configurations and set-up are shown in Figures 42 and 43. A reinforced spar cap segment was also tested, this is configuration C. The reinforcement consisted of adding back-to-back 2024-T3 aluminum angles.

Transverse tension tests were performed to evaluate the offset bending effect of loading due to Poissons effects in the cover and other transverse loads carried into the spar cap. These results are shown in Table 2 and the specimen configurations and set-up are shown in Figures 44 and 45.

Both the interlamina tension and transverse tension strengths demonstrated in a significant reduction when virgin specimens were subjected to GTA No. 1 pre-loading spectrum.

TABLE 1. - INTERLAMINA TENSION TEST RESULTS

Specimen	Configuration*	Prior Load	Test Load lb/Fastener		Remarks
			Initial Failure	Final Failure	
GTA Spar	A	98% DUL	37.5	43.7	Prior Damage Evident
	A	98% DUL	23.7	34.5	
	A	98% DUL	-31.2	-31.2	
Virgin Spar	A	None	88.7	88.7	–
	A	GTA Pre-loading	52.8	56.4	–
	B	None	75.7	75.7	L.E.*** Attached
	C	None	171.6	171.6**	Reinforced

*See Figure 42
**Failure in Skin
***Leading Edge

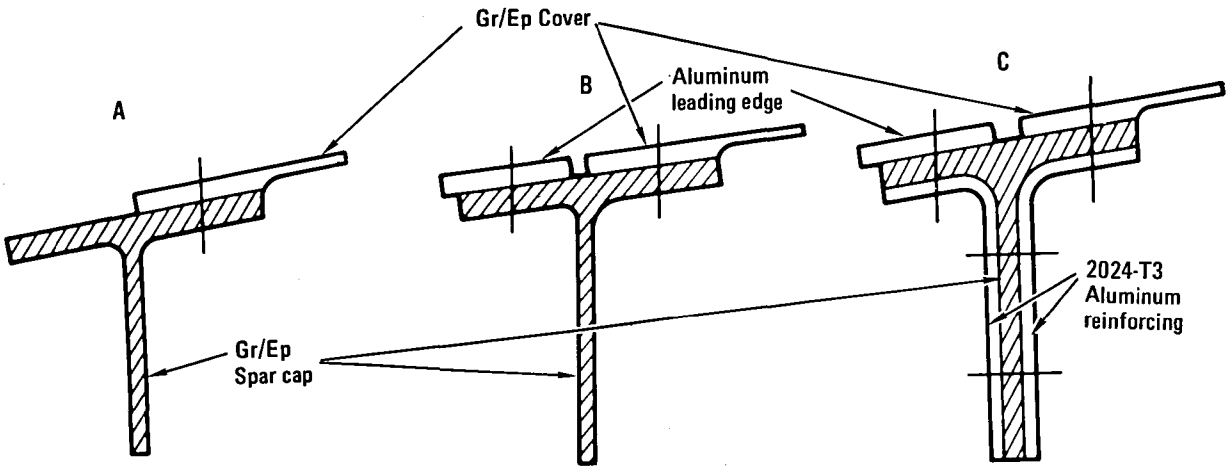

Figure 42. - Interlamina tension specimen configurations.

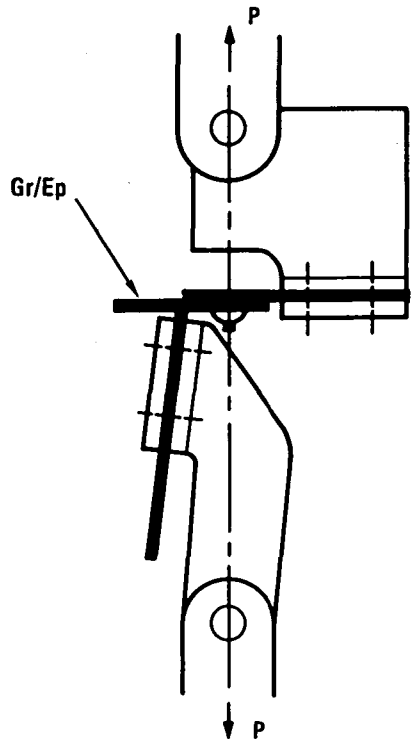

Figure 43. - Interlamina tension test setup.

TABLE 2. - TRANSVERSE TENSION TEST RESULTS

Specimen	Configuration*	Test Load (lb/in.)	Remarks
GTA	A	256	–
Virgin	A	445	–
Virgin	B	667	Reinforced
Virgin	A	225	GTA No. 1 Pre-loading

*See Figure 44

An inplane shear test was performed to verify the inplane load transfer capability of the cover-to-spar cap joint. This test demonstrated a strength of 7,250 pounds for a six-fastener length of spar cap and cover. The design allowable used in this location was 900 pounds/fastener (5400 pounds for six fasteners).

A section of rib cap was cut from the left hand cap of the VSS 171.42 rib toward the rear spar. Visual and C-scan inspection showed no damage in this section. Crippling tests were performed on two sections from this rib cap. The set-up is shown in Figure 46. Failure occurred at 7,110 pounds and 7,980 pounds. The theoretical crippling load was 6,900 pounds.

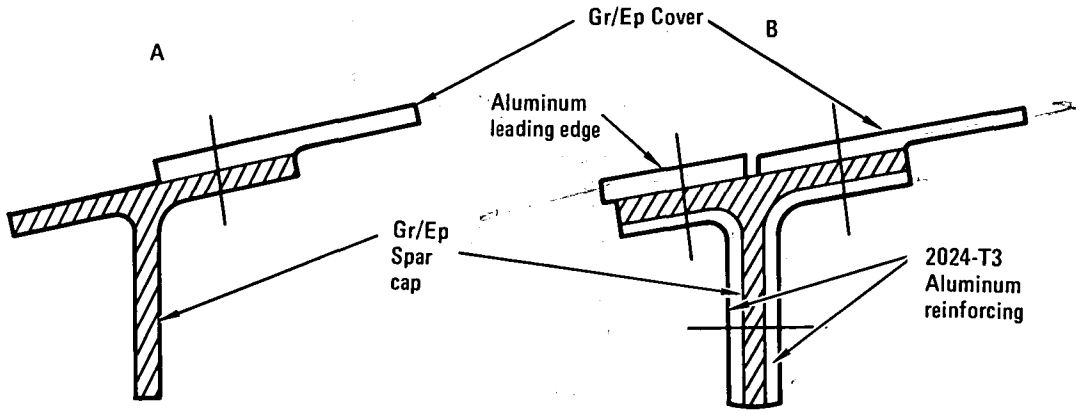

Figure 44. - Transverse tension specimen configurations.

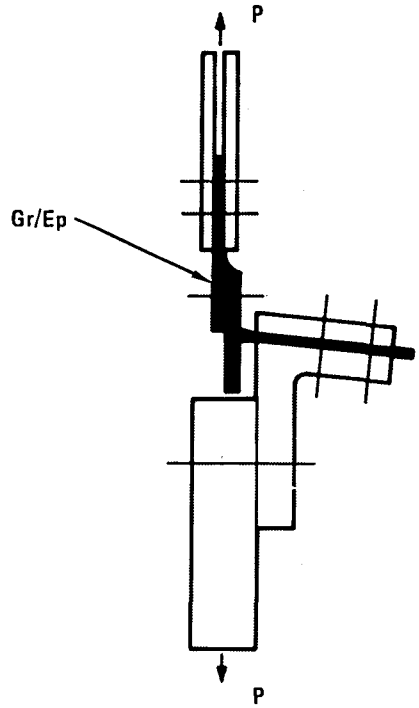

Figure 45. - Transverse tension test setup.

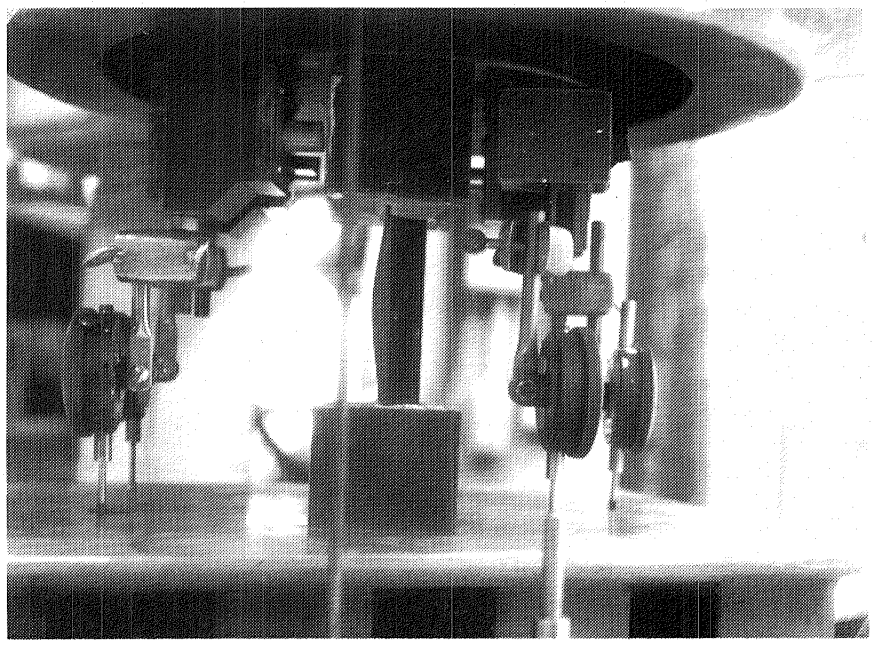

Figure 46. - Rib cap crippling test.

While the test specimens failure modes were not identical to the GTA failure mode they were similar enough to conclude that the GTA failure mode was due to a combination of loads which applied interlamina tension and bending to the spar cap. The tests showed that the spar cap had very low strength capability in interlamina tension and that a low cycle high load fatigue spectrum could cause a significant drop in strength.

3.2 Ground Test Article No. 2

3.2.1 Reinforcement of Ground Test Article Number 2.-It was decided to preform a 'production line' fix on the second fin box to preclude the types of failures encountered with GTA No. 1.

The failure investigation on GTA No. 1 showed that the front spar caps failed, the rib to front spar web attachment angles debonded from the spar web and the cover hat stiffeners adjacent to the front spar in the outboard bays debonded.

The configuration of the spar cap in the region where the failure initiated is shown in Figure 37. In order to provide more strength for

out-of-plane loads, the existing spar caps were reinforced with formed aluminum angles from root to tip. Figure 47 shows the configuration of the angles which are 0.063 in. thick 2024-T3 material. The angles were installed in short lengths (approximately 3 inch) to minimize their picking up axial load.

The ribs are attached to the front spar web through a cocured graphite/epoxy tee. At the rear spar the ribs are attached through aluminum angles which are located and mechanically attached on assembly. A secondary failure on GTA No. 1 involved the separation of the cocured graphite/epoxy tee on the front spar. These tees were reinforced with aluminum angles as shown in Figure 48. The angles are 0.063 in. thick 2024-T3 mechanically attached to the web.

The trapezoidal skin panels adjacent to the front spar in the 10-ply skin area above VSS 248 buckle in shear below limit load. A typical panel is shown in Figure 41. During the failure sequence on GTA No. 1 the stiffeners adjacent to the front spar debonded primarily along the forward flanges in the 10-ply area. The skin was too thin to countersink for fasteners to preclude the debonding of the skin and stiffener in the run-out bays. For the test article 0.032 aluminum doublers were bonded and mechanically attached to both covers locally as shown in Figure 49. These doublers were dimpled at the front spar cap to fit the existing countersinks. The doublers also were countersunk, for the 5/32 inches diameter HL11 fasteners installed along the stiffener flanges.

3.2.2 Test Set-up.-The test set-up and the applied loads were identical to those for GTA #1 as described in section 2. Some changes were made in strain gage locations based on the results from GTA #1. These changes were only to the

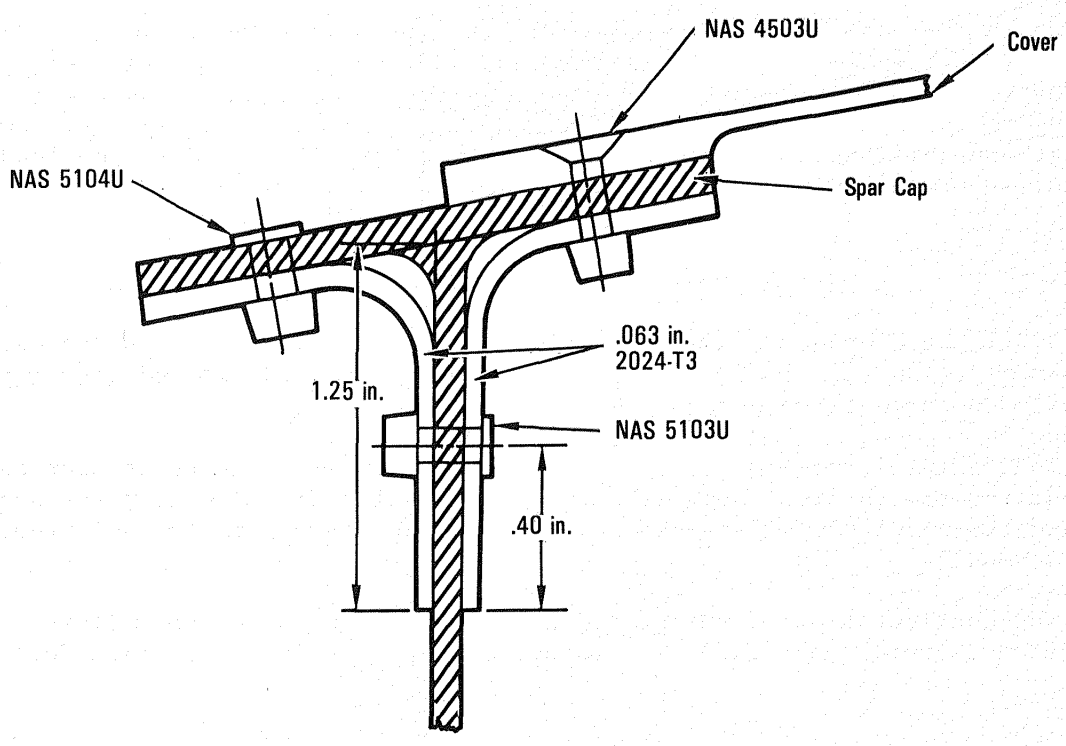

Figure 47. - Spar cap reinforcement.

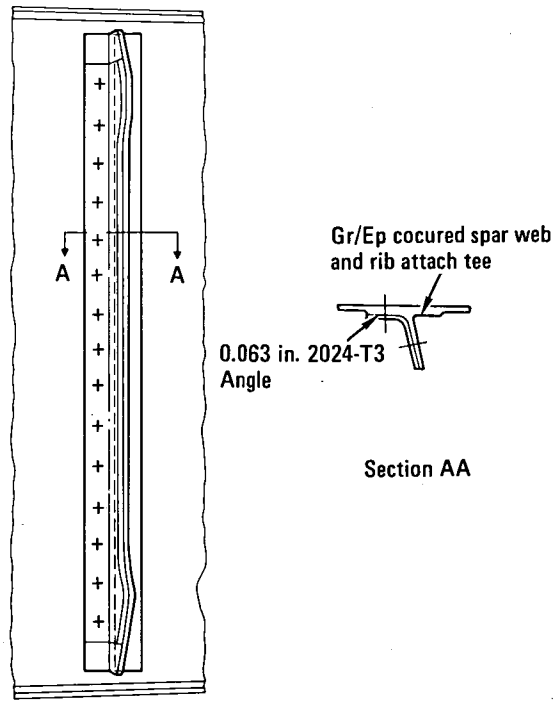

Figure 48. - Front spar to rib attachment reinforcement.

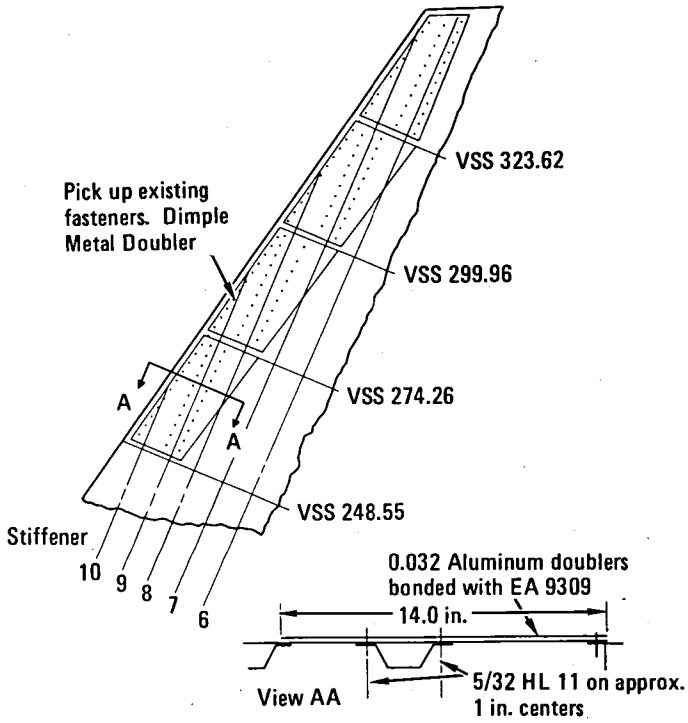

Figure 49. - Cover doublers.

covers and spars. The cover and spar strain gage locations for GTA #2 are shown in Figures 50 and 51.

3.2.3 Static Test.-Prior to static testing a strain survey to 50 percent Design Ultimate Load (DUL) was performed. The fin box was found to be responding as anticipated. The fin box was mounted horizontally with the right hand surface down. Static tests were all performed with jacks pulling down so the right hand surface was in compression and the left hand surface was in tension. For damage tolerance and fail-safe testing all loading was fully reversed so both surfaces saw the same tension and compression loading.

Testing commenced by loading to Design Limit Load. Data from selected key strain gages were reviewed to establish that the fin box was behaving as anticipated. The fin box was then loaded to 106 percent DUL and then back to zero. The 106 percent DUL was to cover the estimated environmental degradation effects as discussed in Section 2.5.

The maximum cover axial strain was about 2800 μin/in with local strains in a buckled area at about 4000 μin/in. The right hand cover 16-ply skin between VSS 121 and VSS 97 near the rear spar buckled in compression at 82 percent DUL which was consistent with the PRVT static cover tests where buckling initiated between 78 and 108 percent under uniaxial loading. The trapezoidal cover panels in the lower 14-ply bay were instrumented with back-to-back shear rosettes. Buckling occurred on both tension and compression covers.

There was no evidence of any buckling on the spar webs. The lower six access holes on the front spar were reinforced in the same manner as on GTA No. 1. Shear strains in the front spar webs were fairly even, ranging from 3600 μin/in to 4600 μin/in. The rear spar shear strains were low, with a maximum of 1600 μin/in.

A post-test inspection revealed no damage or loose fasteners.

4. DAMAGE TOLERANCE TESTING

Once the static testing was completed GTA No. 2 was prepared for the damage tolerance testing.

The load cells and jacks required changing for the damage tolerance test because of the lower loads applied during the cyclic tests, and because the loads were fully reversed through tension and compression. The load cells thus required a greater sensitivity and jacks a longer stroke.

The fatigue spectrum employed is contained in Table 3. The applied loads are specified as percent values of Condition 59 limit load levels; the frequency of occurrence of these loads is defined by flight intervals throughout the 36,000 flight lifetime. The loads were applied as fully-reversed load cycles. This fatigue spectrum is a little more severe than that applied to the L-1011 fatigue test article. The final flight loads included the application of design limit load with a 1.06 factor (see paragraph 2.5).

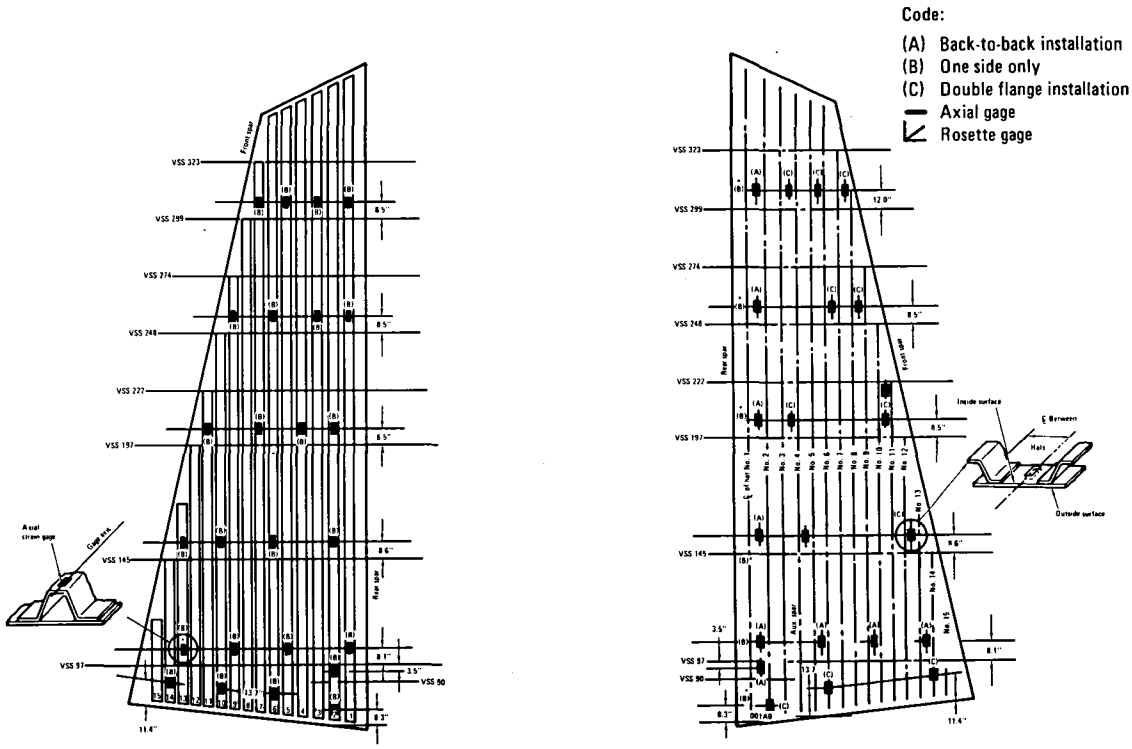

RIGHT SIDE

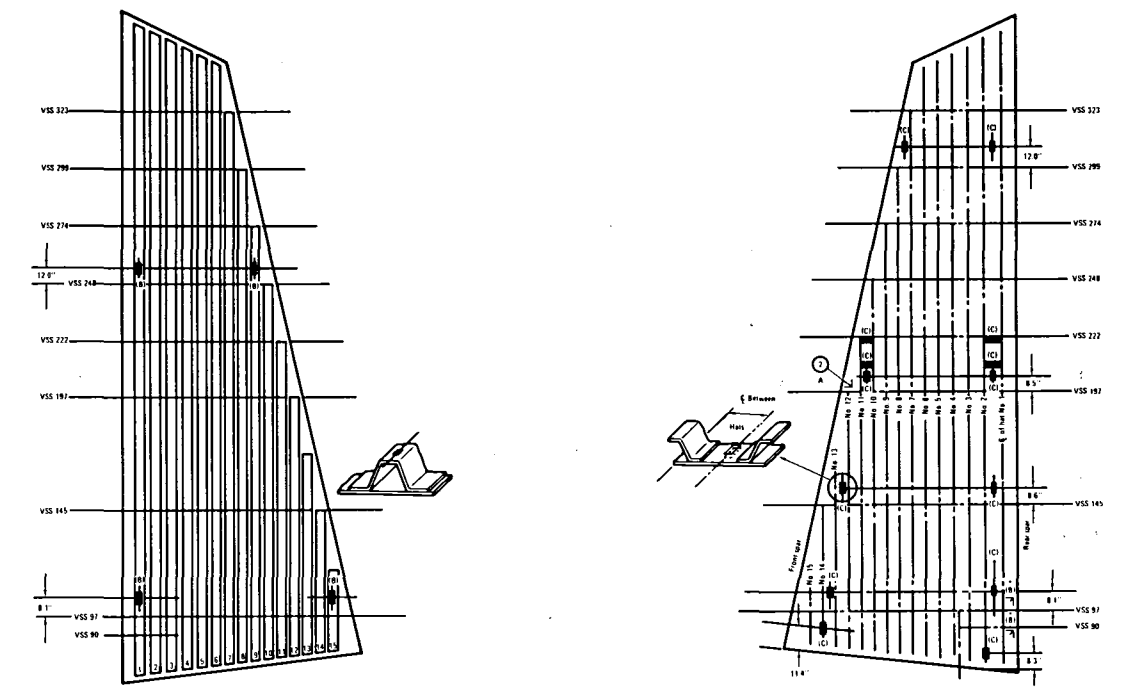

LEFT SIDE

Figure 50. - Strain gage installation, right and left covers GTA No. 2.

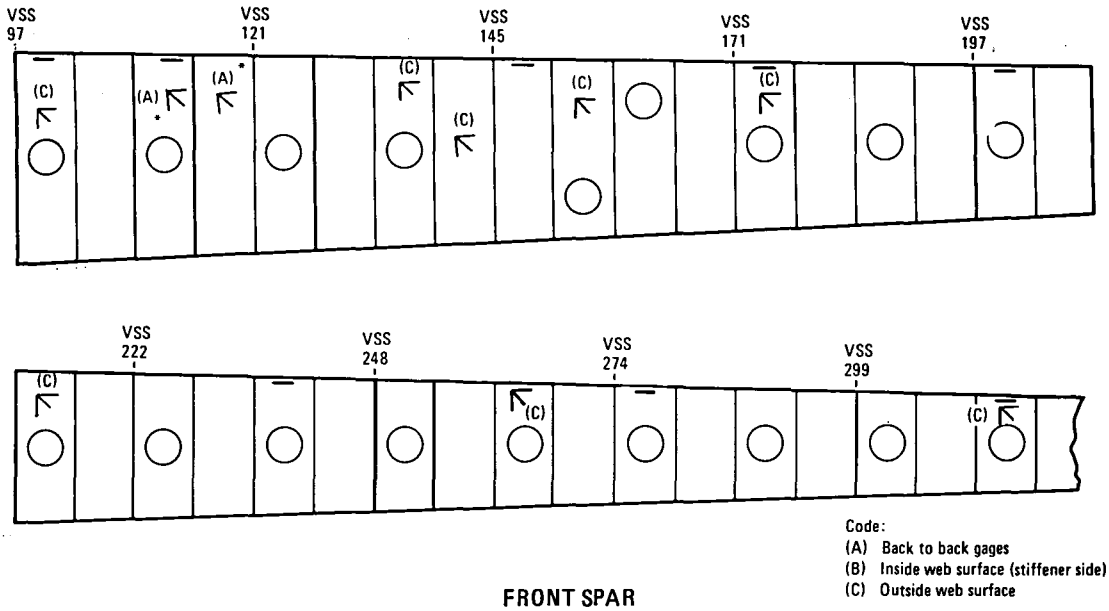

FRONT SPAR

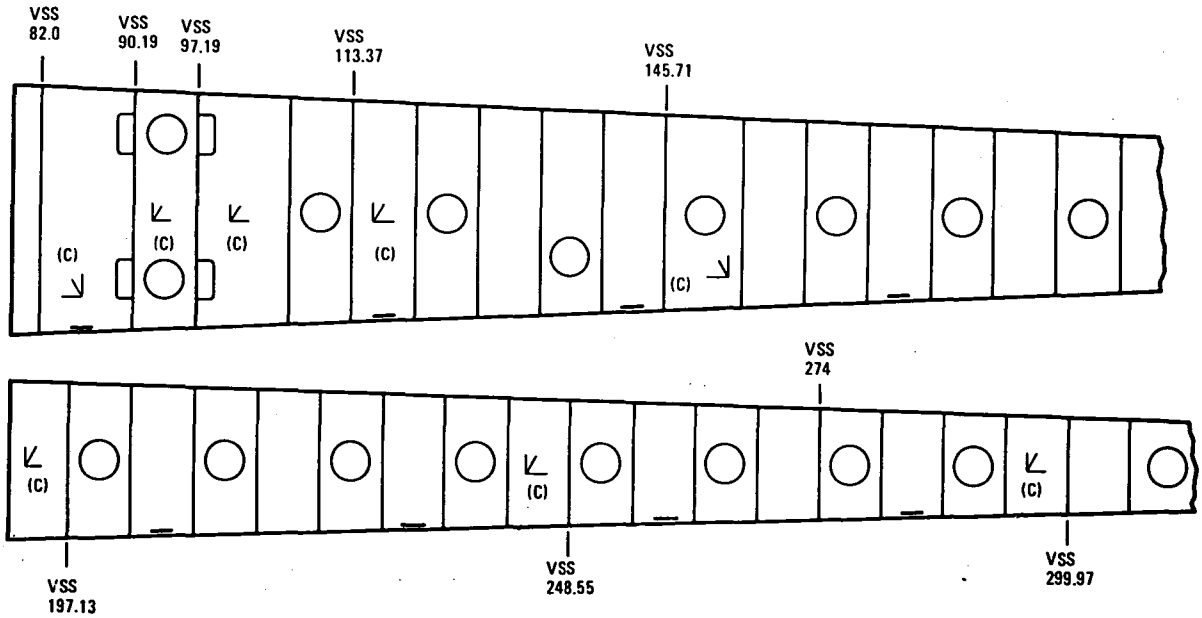

REAR SPAR

Figure 51. - Strain gate installation, front and rear spar GTA No. 2

TABLE 3. - DAMAGE TOLERANCE EVALUATION FATIGUE SPECTRUM

% Limit Load	N	ΣN	Flight						
			1	36	360	1800	9000	18000	36000
15	166000	197020	4	22					
23	24860	31020		24	8	3			
31	4328	6160		4	3	1	2		
38	1279	1832		1	2	3	4	1	1
46	328	553			3	1	2		
54	134	225			1	1	3	1	
62	43	91				2		1	1
69	28	48				1	2		
77	9	20					2		1
81	3	11						1	1
85	3	8						1	1
88	3	5						1	1
92	1	2							1
*106	1	1							1
	Count		4	51	17	12	15	6	8
	Multiplier		36000	1000	100	20	4	2	1

*Environmental factor applied to limit load only.

4.1 Impact Damage

The impacting for the damage tolerance evaluation was performed at the locations shown on Figure 52. Impacting was performed using a calibrated impactor gun as shown on Figure 53. The impactor was a one in. diameter steel ball. The initial impact energy levels were determined from trials on ancillary test components of similar configuration. All cover impacts were over stiffener flanges in the most critical areas for each skin thickness.

Impact No. 1 was in the 16-ply skin area near the aft region of the cover root end. One impact at 13.33 ft.-lb was sufficient to cause visible surface damage.

Impact No. 2 was in the 14-ply skin area. Four impacts were required to obtain visible damage. The first impact was a 13.33 ft.-lb. Some damage was evident ultrasonically. A second impact at 8.64 ft.-lb. showed no evidence of change ultrasonically. A third impact, now back at 13.33 ft.-lb. gave no visible damage but increased the damage area determined ultrasonically. A fourth impact was made, but at an energy level of 18.95 ft.-lb. Visible penetration through the thickness occurred.

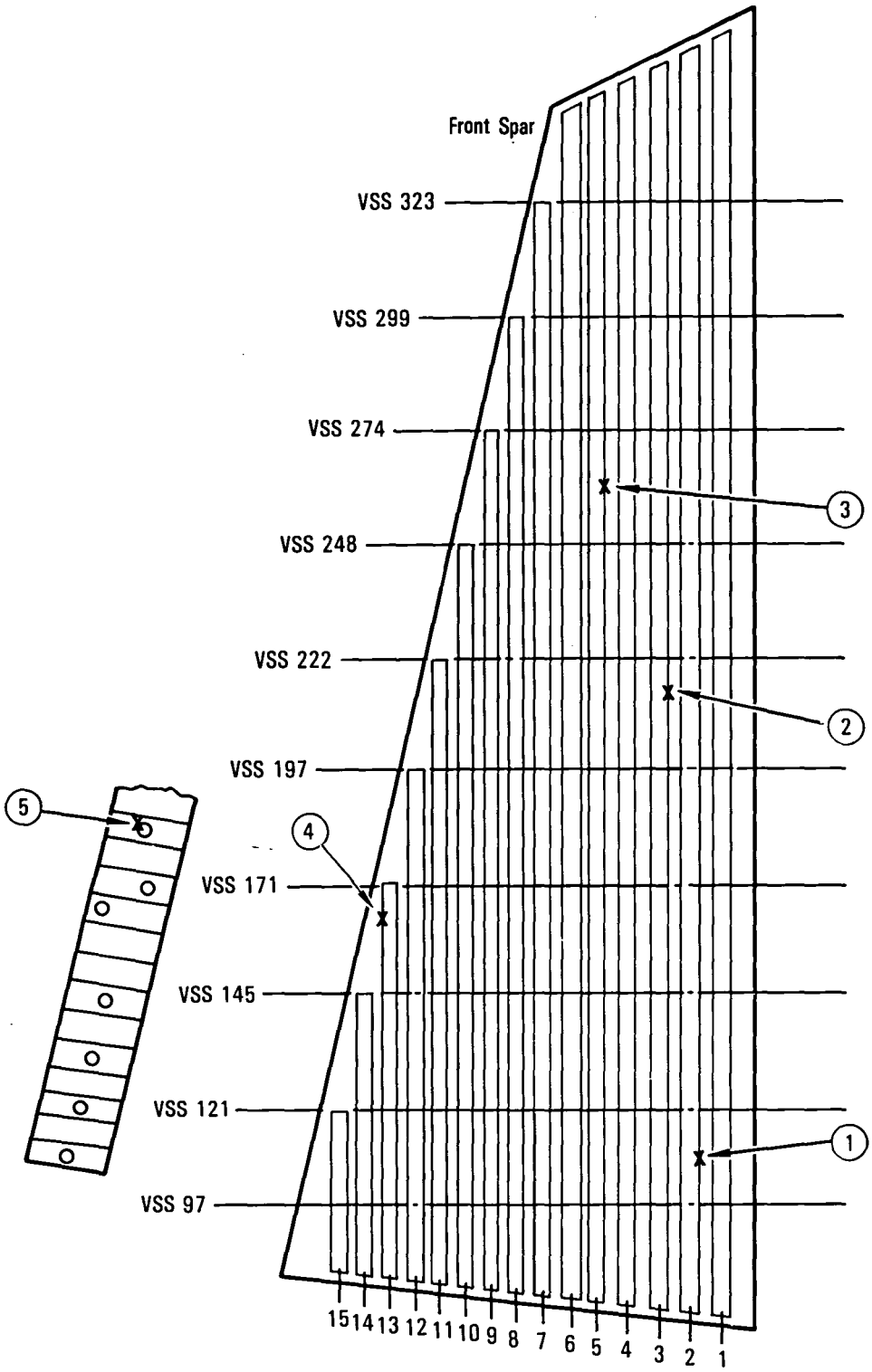

Figure 52. - Impact damage locations.

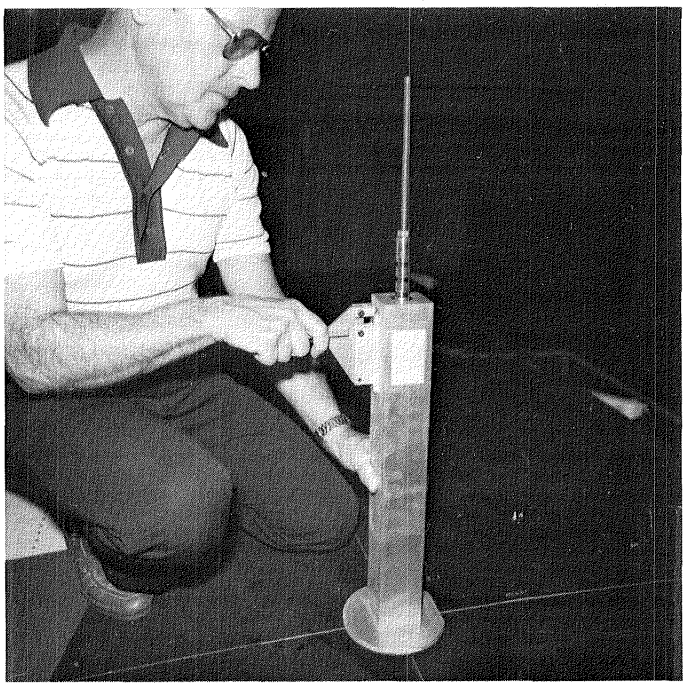

Figure 53. - Impactor gun.

Impact No. 3 was in the 10-ply skin area. Because the impact in the 14-ply area required more energy than the calibration had indicated, this area was impacted at 13.33 ft.-lb. also. One impact caused visible surface damage.

Impact No. 4 was in the 16-ply skin area adjacent to the front spar. Because this area was very rigid it was anticipated that lower impact levels would cause damage. However after six impacts at 8.64 ft.-lb. no visible damage occurred internally or externally, and the ultrasonically determined damage area remained essentially unchanged after the first impact. Two more impacts at the higher energy level of 13.33 ft.-lb. again made little difference. There was some evidence of hat flange skin separation extending to the rib about three inches away. It was decided to do no more impacting in this area and to show that nonvisible damage would not grow to catastrophic proportions during a lifetime of loading.

Impact No. 5 was on the front spar web at the lowermost unreinforced access hole. The first impact at 7.99 ft.-lb. gave no visible damage. A second impact of 12.52 ft.-lb. gave visible delamination of the surface and in the edge of the access hole.

Damage tolerance testing commenced. At the completion of each one-quarter lifetime (9,000 flights) of fatigue loading the impacted areas were inspected ultrasonically and damage growth, if any, marked on the part. Figures 54 through 58 show the damage and growth at each of the five locations. Most growth occurred during the first half lifetime of fatigue cycling and could only be determined ultrasonically.

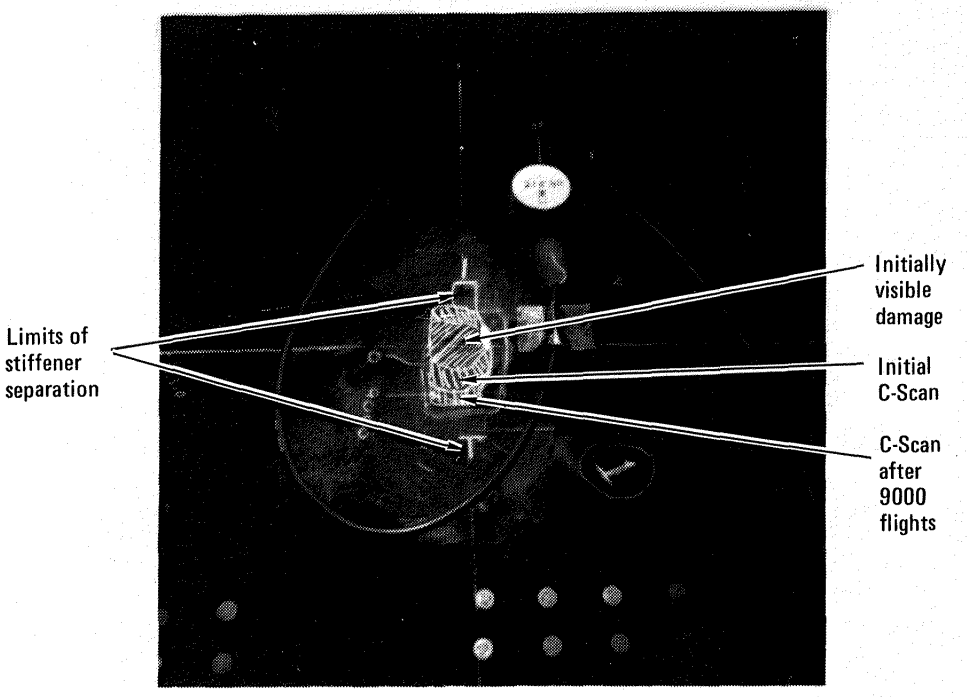

Figure 54. - Location No. 1 damage growth.

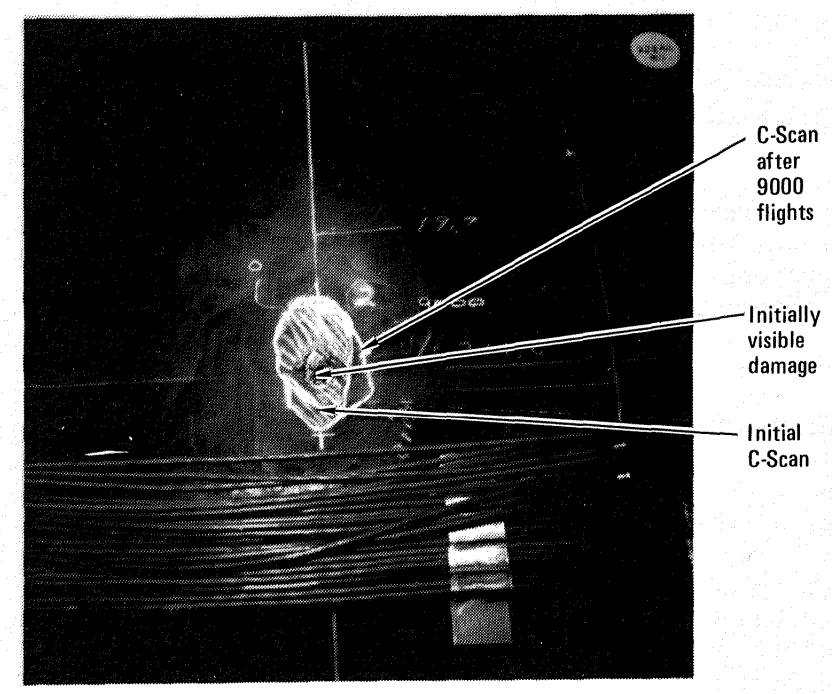

Figure 55. - Location No. 2 damage growth.

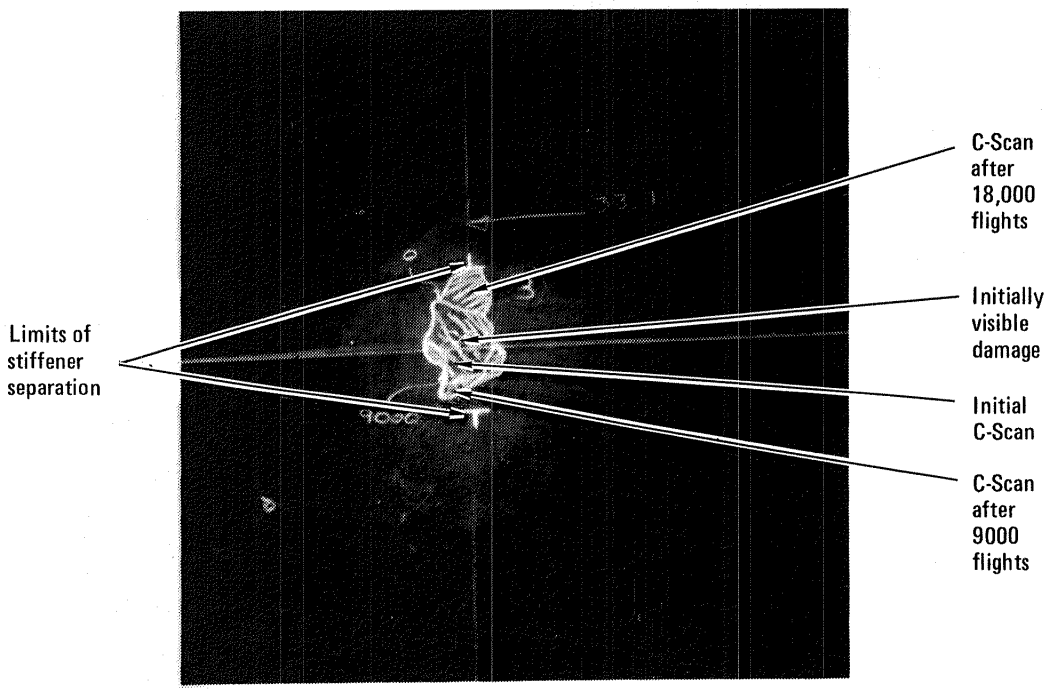

Figure 56. - Location No. 3 damage growth.

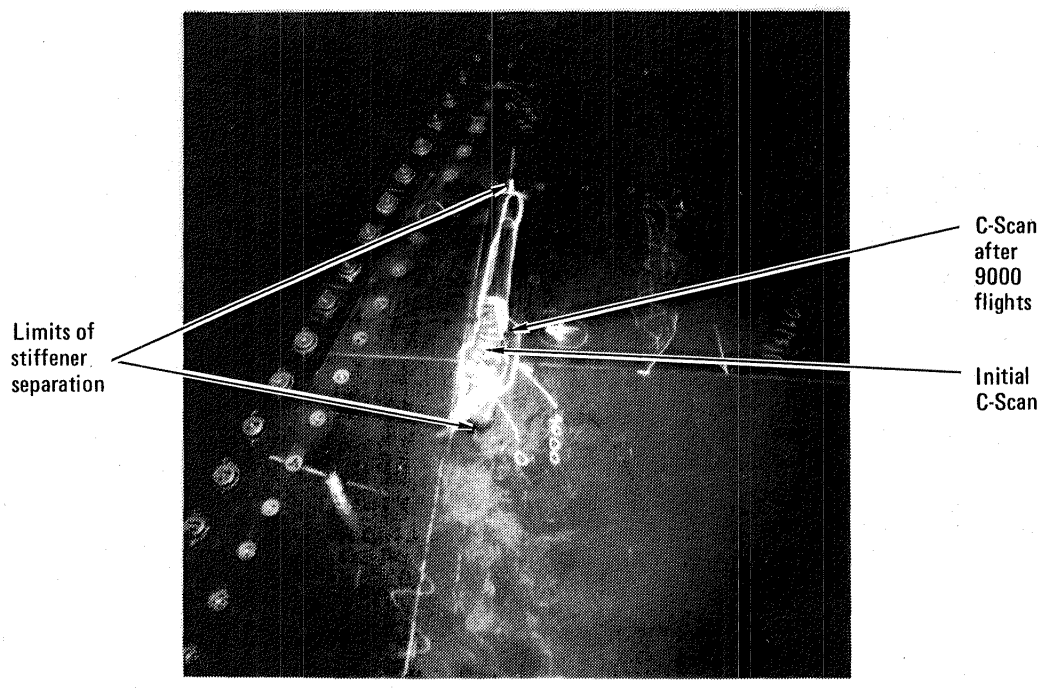

Figure 57. - Location No. 4 damage growth.

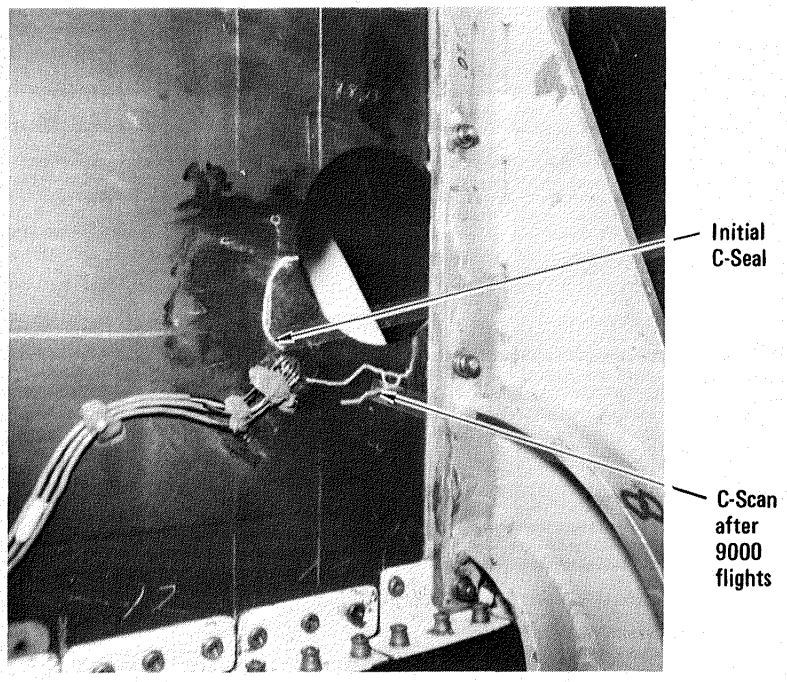

Figure 58. - Location No. 5 damage growth.

4.2 Discrete Damage Test and Repair

At the completion of one lifetime, simulated lightning strike damage was inflicted to the fin cover. The area selected was considered to be the most critical for large area damage. An area on the left hand cover between VSS 97.19 and VSS 121.1, approximately 12 by 4 in. and at a 45^{o} angle to the rear spar, was damaged by impacting to obtain delaminations. A hole was then burned through the skin using an electric arc from a 3/16 in. diameter welding rod. The delaminated area was then burned with oxygen/acetylene flame torch to char the outer plies.

Figure 59 shows the hole being burned through the cover and Figure 60 shows the overall charring operation. The resulting overall damage is shown in Figure 61.

The fin box was then loaded to 1.06 Design Limit Load in both directions, so the damaged cover was loaded once in tension and once in compression. A post test ultrasonic inspection showed no growth in any of the damage.

The discrete source damage was then cleaned up for repair. The burned through hole was surrounded by badly charred resin and required opening up to a 2 in. by 2 in. hole. The hole was filled with a room temperature setting compound and a precured block of graphite/epoxy of the same thickness. The surface of the damaged area was cleaned with Scotchbrite and then wiped with

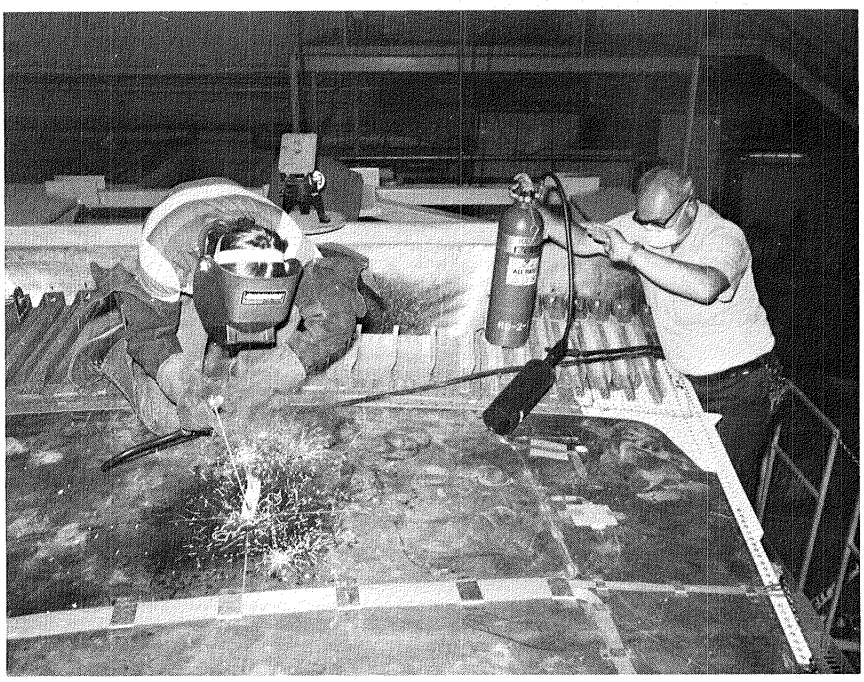

Figure 59. - Burning hole with electric arc welding rod.

Figure 60. - Charring with oxygen/acetylene flame torch.

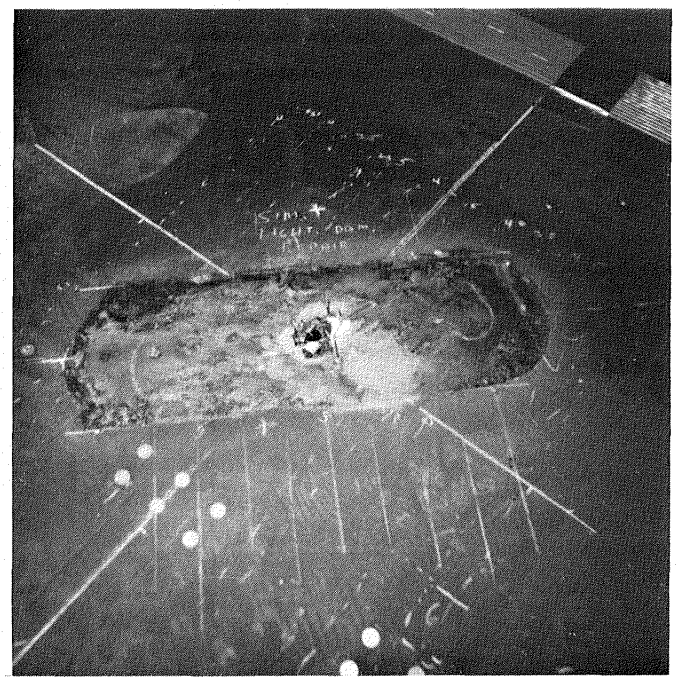

Figure 61. - Overall simulated lightning damage.

MEK. The externally bonded repair is shown schematically on Figure 62 and consisted of five precured layers of graphite/epoxy. The layers are identified on Figure 62 as (1) and (2). (1) is +45/-45/-45/+45 and (2) is 0_3. The (1) layers were cut from an existing panel fabricated from T300/5208.[3] The (2) layers were laid up and cured from AS4/3502 material. AS4/3502 was used as there was no T300/5208 available. A layer of M329 adhesive was placed on the fin surface and between each precured layer. The assembly was covered with porous Armalon and A 4000 and vacuum bagged with a nylon bag (see Figure 63). After a vacuum and leak check heater blankets and insulation were applied as shown in Figure 64. Vacuum was applied and the patch was heated to 350°F for one hour then cooled to 180°F and vacuum removed. Upon removal of the heater blanket and vacuum bag it was apparent that the middle area of the patch had overheated. The vacuum bag had melted to the silicone rubber heating blanket. The top layer of the five layers of patch material was buckled upwards from the skin contour. The edges all appeared well bonded. The top three layers were removed. The two bottom layers were well bonded and were retained.

Three new stacks were prepared and bonded in place. The heat up rate was reduced to 3°F/min from the recommended 6°F/min. The edges of the repair only reached 273-276°F. When the center reached 355°F, the cure was extended to two hours based on the vendor recommendation. Full vacuum was held throughout the cure.

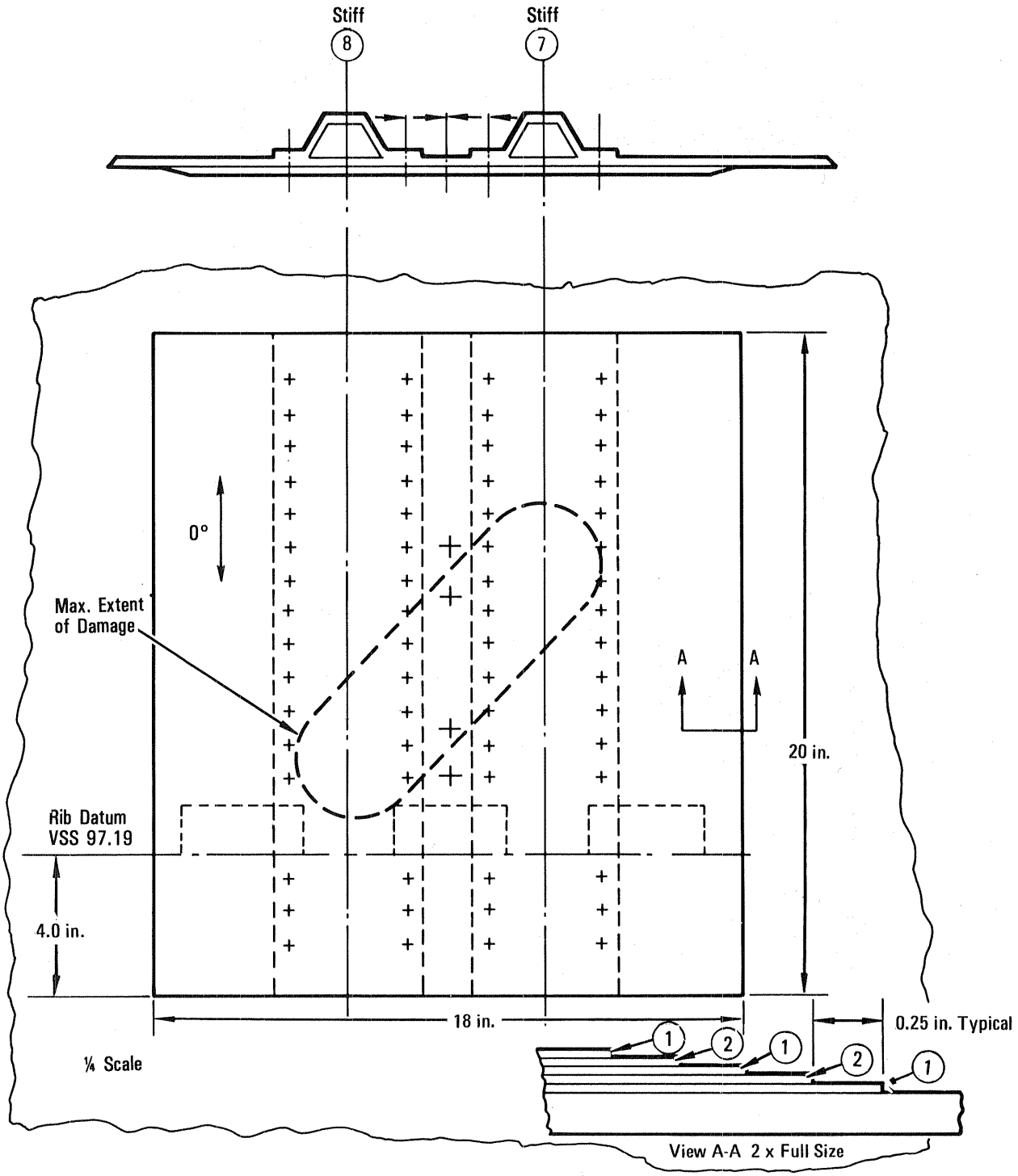

Figure 62. - Damage repair.

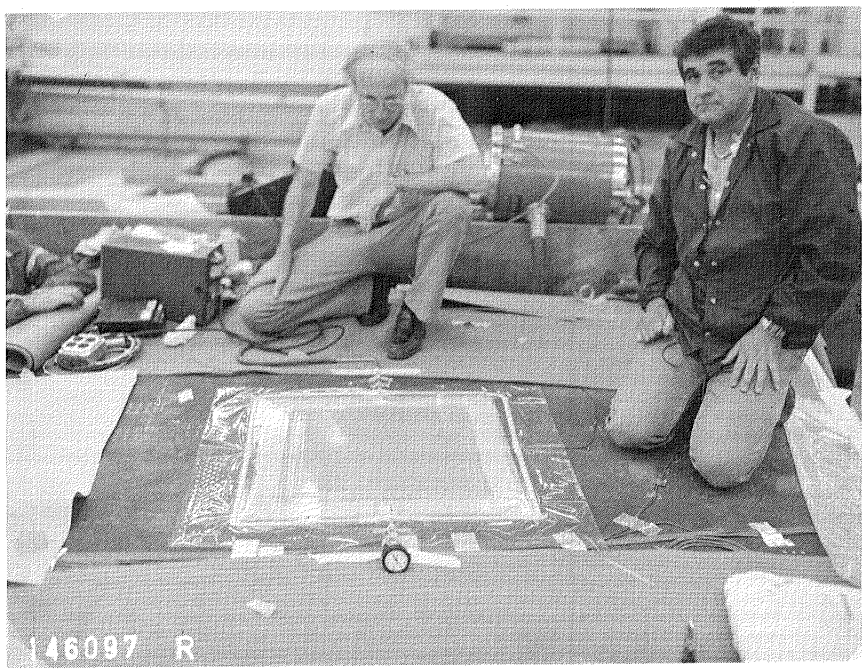

Figure 63. - Repair in place and bagged.

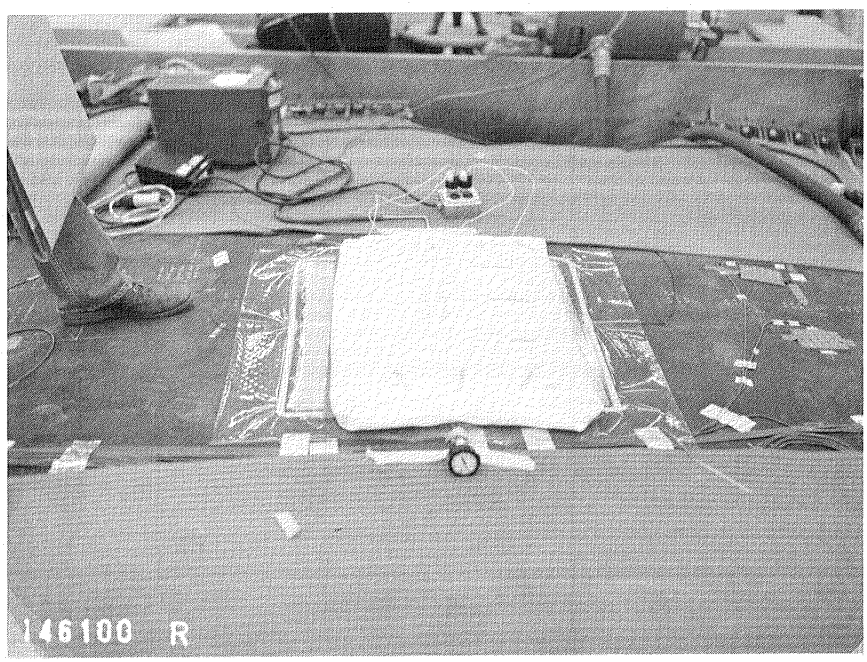

Figure 64. - Heater blanket in place.

Visual inspection of the completed repair showed no discrepancies. Ultrasonic inspection of the patch indicated distributed porosity in the adhesive. The porosity had been anticipated based on previous patch tests and was acceptable. The repair technique was based on a method developed under another NASA contract with Lockheed; NAS1-15269, "Development, Demonstration, and Verification of Repair Techniques and Processes for Graphite/Epoxy Structures for Commercial Transport Aircraft."

A second lifetime of damage tolerance testing followed. On completion of this second lifetime of fatigue cycling an ultrasonic inspection revealed no change in any of the damage areas and no effect on the repair.

The fin box was then prepared for static test to determine its residual strength. Failure was anticipated in one of several locations. The first location was the front spar web above VSS 171 and would be preceded by shear buckling of the web. The second location was in the covers between VSS 197 and VSS 222 adjacent to the front spar on either surface. It would be preceded by shear buckling. The final location was in the right hand cover toward the rear spar and would be preceded by compression buckling. The exact location would depend on which area had the weakest interlamina strength between the stiffener and the skin or web. Failure was expected to occur at approximately 120 percent Design Ultimate Load.

4.3 Residual Static Strength Test

The testing of GTA No. 2 was completed on July 8, 1982 when the static test to failure was performed. Failure occurred at 119.7% DUL in the left hand (tension) cover near the front spar and between ribs VSS 248 and 222. Figure 65 shows the fin just prior to failure and Figure 66 shows the fin just as failure occurred.

A review of the high speed movies of the test showed that the failure initiated at the lower end of the bay adjacent to the VSS 222 rib and then propagated up to VSS 248.

A post test inspection showed that the damage in the left hand cover extended from VSS 248 down to VSS 145 and from stiffener No. 9 to stiffener No. 11. The visible surface damage to the cover is shown in Figures 67 and 68. Figure 67 shows the area by VSS 248 where the outer skin plies delaminated. Figure 68 shows surface ply delamination at VSS 197. The rib caps in this area were also damaged. Figure 69 shows the broken left hand cap at VSS 222.84. The deformations resulting from the failure also failed the inner right hand cap of the VSS 222 rib at a truss member. The left hand cap of rib VSS 197, VSS 171 and VSS 145 also failed. Figure 70 shows the broken inner flange of the left hand rib cap at VSS 145. The rib cap failures were due to induced deformations when the skin and stiffener separation emanated down the cover.

The initial failure was caused by high interlaminar tension stresses induced by shear buckling of the skin panel between VSS 248 and VSS 222 and between the front spar and stiffener No. 10. Buckling initiated about design

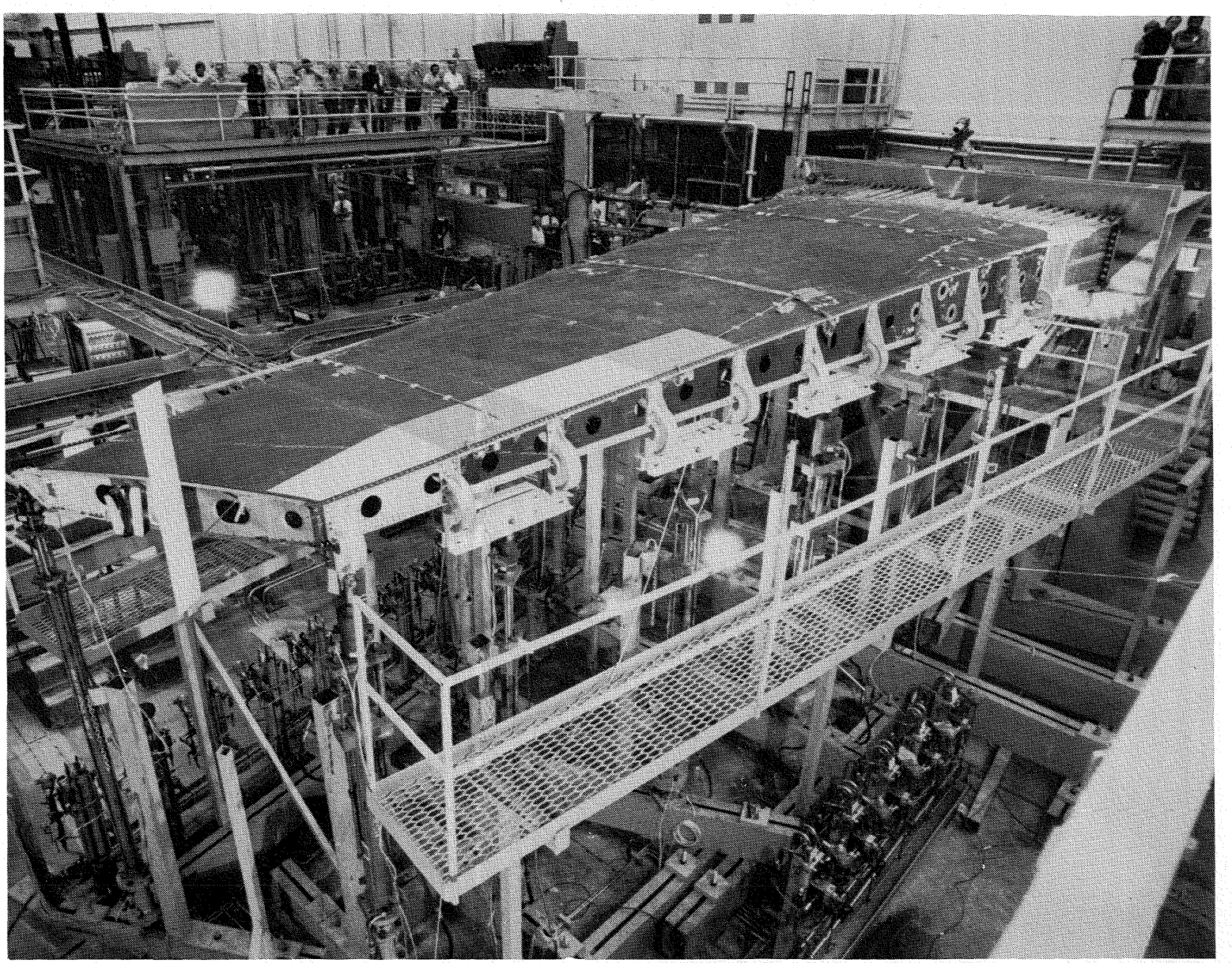

Figure 65. - Fin box just prior to failure.

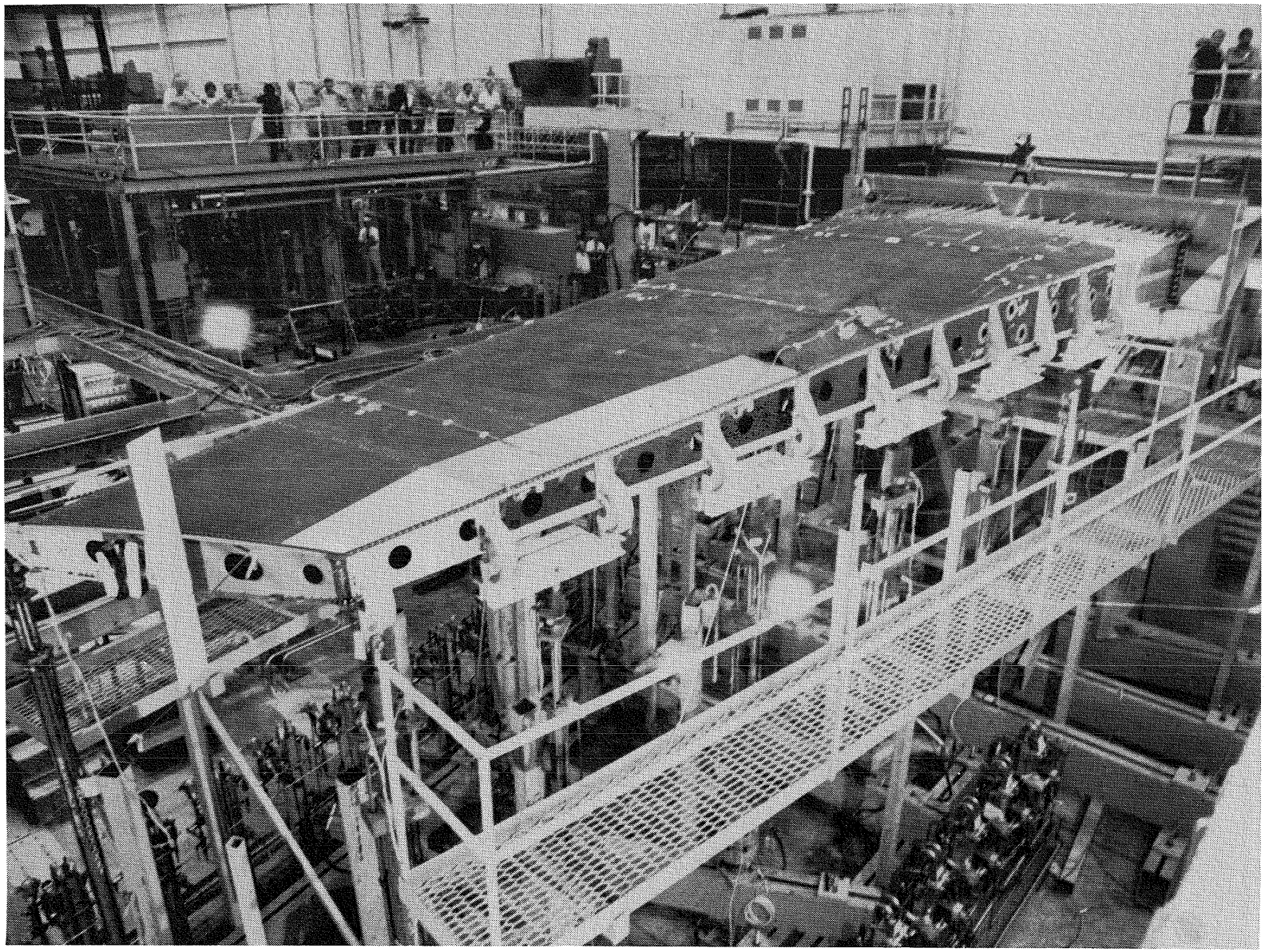

Figure 66. - Fin box at moment of failure.

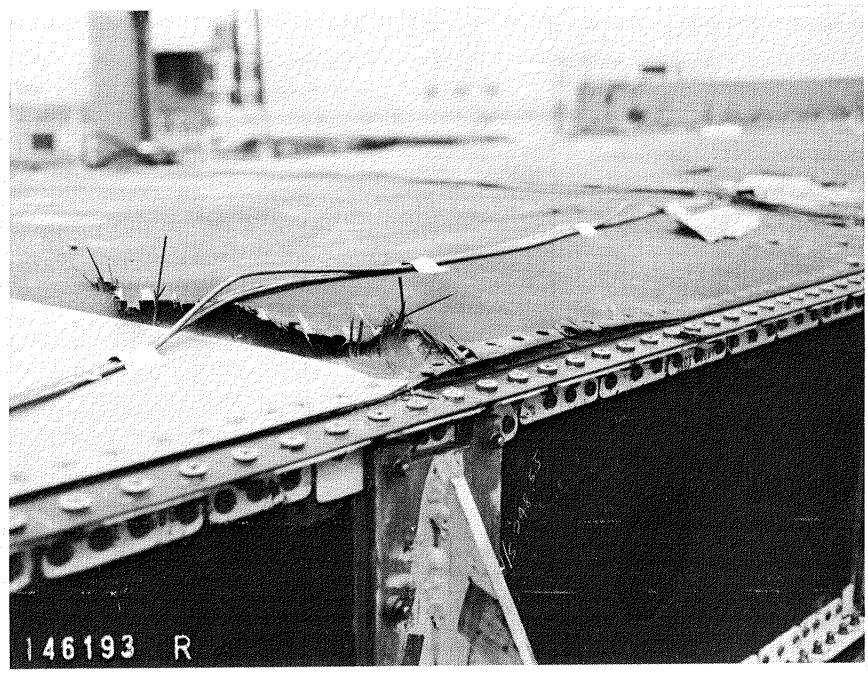

Figure 67. - Cover failure in vicinity of VSS 248.

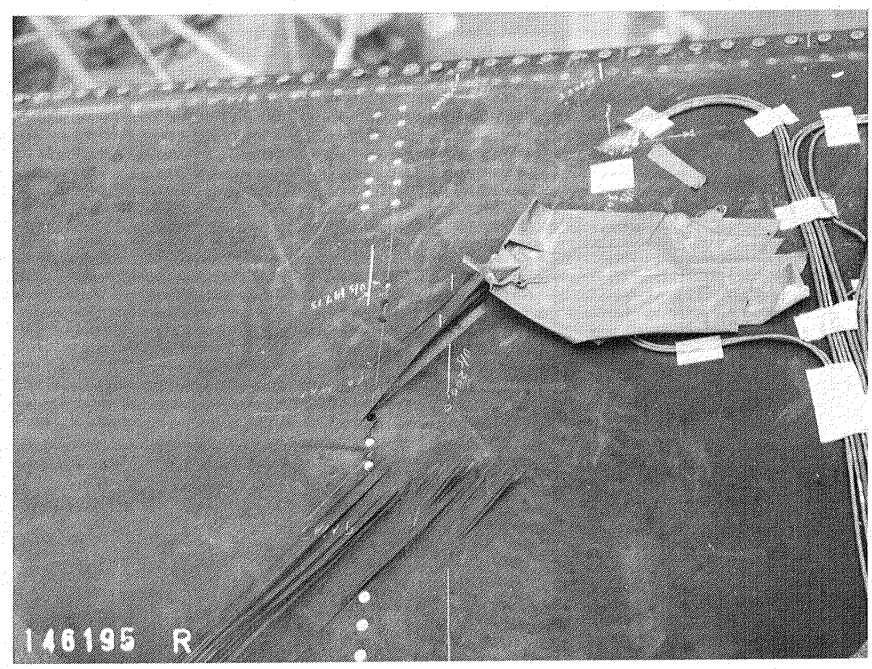

Figure 68. - Cover failure in vicinity of VSS 197.50.

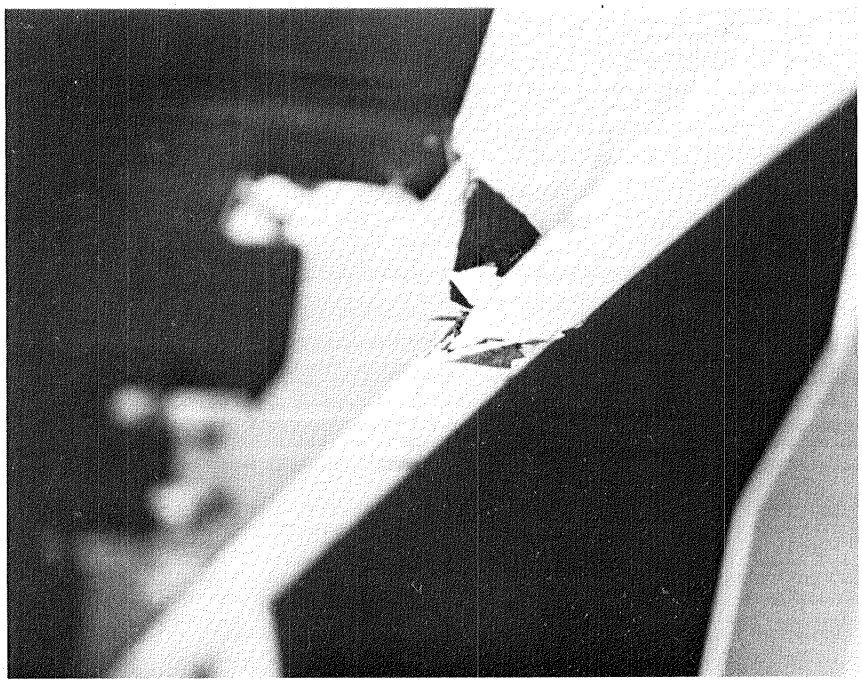

Figure 69. - Broken left hand rib cap at VSS 222.84.

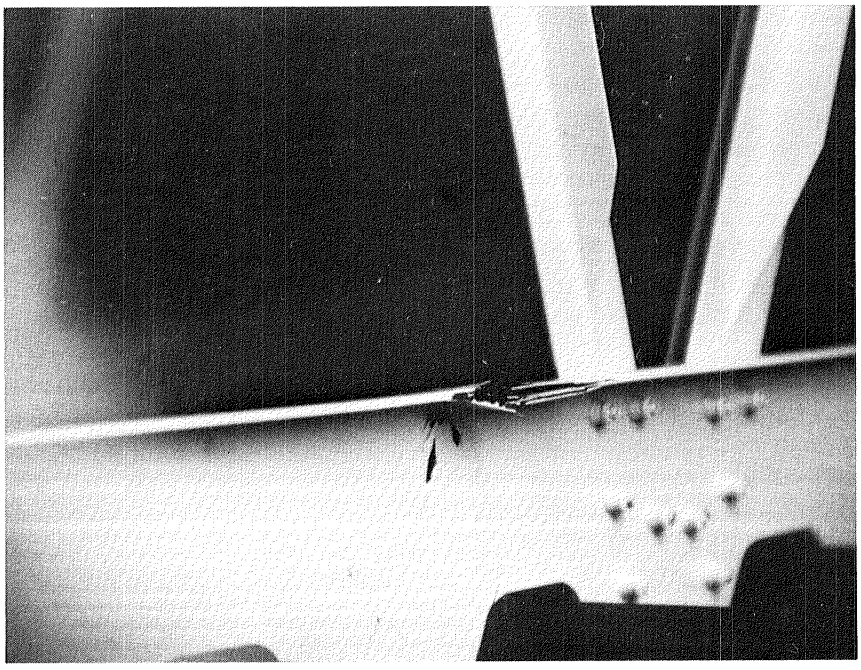

Figure 70. - Left hand rib cap flange failure at VSS 145.71.

limit load. Shear buckling occurred on the tension surface before it occurred on the compression surface. This appears to be due to the interaction of shear and Poisson induced compression strains in the chordwise direction being more severe than the shear and spanwise compression on the other surface. This condition would be greatly changed if the cover contained one or two 90^{o} plies.

The compression surface started to buckle at about 80 percent DUL and by 110 percent DUL much of the skin between VSS 121 and VSS 97.19 was buckled. No buckling occurred in the spar webs.

The strains at 106 percent DUL compared very well with those from the static test performed on GTA No. 2 on April 7, 1982, even in the locations where the strains were non-linear due to buckling. This indicates that no degradation occurred during the damage tolerance testing.

The failures were very similar to those which occurred on GTA No. 1. The spar cap and rib to spar web reinforcement prevented failures in those locations and the cover doublers moved the failure initiation bay down to the first unreinforced bay. The conclusion is that the failure in both GTA No. 1 and GTA No. 2 was due to interlamina tension loading caused by shear buckling of the cover strip panel between the front spar cap and the first hat stiffener. In GTA No. 1 the failure apparently initiated in the spar cap and in GTA No. 2 failure initiated at the skin to stiffener interface near VSS 222.

CONCLUSIONS

The first static test uncovered a deficiency in the spar cap design. The cap was not able to carry sufficient unsymmetric out-of-plane load. The second test article was reinforced to preclude the types of failure which occurred in the first test. These reinforcements performed as anticipated and the static test to 106 percent DUL was successfully completed with no failures.

The damage tolerance of the fin box was demonstrated. Some growth of the intentional impact damage occurred, primarily in the first half lifetime of spectrum fatigue loading. No growth occurred during the second lifetime.

The fail-safe aspect of the design was demonstrated when the box sustained ±106 percent DLL with major damage in one cover. This damage was repaired using in-service repair techniques and the repair was verified by withstanding one lifetime of spectrum fatigue testing.

The fin box was tested to destruction and failure occurred just below 120 percent DUL. The failure was not influenced by the impact damage or by the repair.

REFERENCES

1. NASA CR 165634 Phase II - Final Report Design and Analysis, April 1981.

1. Report No.	2. Government Accession No.	3. Recipient's Catalog No.
NASA CR 166015		

4. Title and Subtitle	5. Report Date
ADVANCED MANUFACTURING DEVELOPMENT OF A COMPOSITE EMPENNAGE COMPONENT FOR L-1011 AIRCRAFT PHASE V, FINAL REPORT, FULL SCALE GROUND TEST	December 1982
	6. Performing Organization Code D76-23
7. Author(s)	8. Performing Organization Report No.
A. Jackson, F. Dorward	LR 30357
	10. Work Unit No.
9. Performing Organization Name and Address	11. Contract or Grant No.
Lockheed Corporation Lockheed-California Company P.O. Box 551 Burbank, California 91520	NAS1-14000
	13. Type of Report and Period Covered
12. Sponsoring Agency Name and Address	Contractor Report
National Aeronautics and Space Administration Washington, DC 20546	14. Sponsoring Agency Code

15. Supplementary Notes

Langley technical monitor: Dr. Herbert A. Leybold

16. Abstract

The activities documented in this report are associated with Phase V of the Advanced Composite Vertical Fin program. This phase included the ground testing of two full-scale components.

The first full scale Ground Test Article (GTA) failed at 98% Design Ultimate Load (DUL) during static test. The failure initiated in the front spar cap in interlamina tension.

The second component GTA #2 was prepared for static and damage tolerance testing. This component was reinforced prior to test to preclude the types of failure encountered on GTA #1. The fin box was then loaded to 106% DUL successfully with no failures. The additional 6% was applied to account for environmental effects which were not simulated.

Following static testing, GTA #2 had deliberate impact damage inflicted at several locations of the cover and the front spar web. One lifetime (36,000 flights) of fully reversed cyclic fatigue loadings was then applied to the fin. Ultrasonic inspection was performed after each quarter lifetime. Some damage growth occurred primarily in the first half lifetime.

After the one lifetime major damage was inflicted in the cover to simulate lightning strike damage and a full cycle of 106% design limit load was applied. Inspection showed no detectable change on any of the damaged areas.

17. Key Words (Suggested by Author(s))	18. Distribution Statement
Composites, Materials, Primary Structure, Testing, Transport Aircraft, Graphite Epoxy	Unclassified - Unlimited

19. Security Classif. (of this report)	20. Security Classif. (of this page)	21. No. of Pages	22. Price
Unclassified	Unclassified	74	

For sale by the National Technical Information Service, Springfield, Virginia 22161

The major damage was then repaired using in-service repair techniques. A second lifetime of cyclic fatigue loadings was then applied. Again, none of the damaged areas grew during this second lifetime.

The fin box was then tested to destruction. The failure occurred at 119.7% DUL in the left-hand (tension) cover.

End of Document